



# Lawrence Berkeley Laboratory

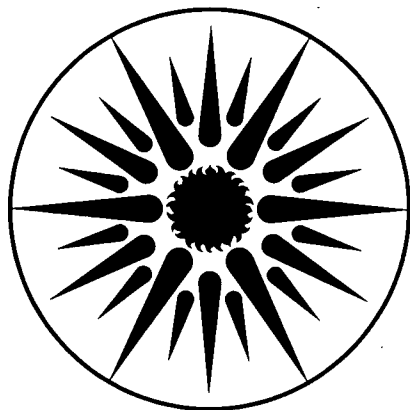
UNIVERSITY OF CALIFORNIA

## ENERGY & ENVIRONMENT DIVISION

**Exploratory Technology Research Program  
for Electrochemical Energy Storage**

**Annual Report for 1991**

June 1992



**ENERGY & ENVIRONMENT  
DIVISION**

REFERENCE COPY  
Does Not  
Circulate

501 Library

LBL-32212  
Copy 1

## **DISCLAIMER**

This document was prepared as an account of work sponsored by the United States Government. While this document is believed to contain correct information, neither the United States Government nor any agency thereof, nor the Regents of the University of California, nor any of their employees, makes any warranty, express or implied, or assumes any legal responsibility for the accuracy, completeness, or usefulness of any information, apparatus, product, or process disclosed, or represents that its use would not infringe privately owned rights. Reference herein to any specific commercial product, process, or service by its trade name, trademark, manufacturer, or otherwise, does not necessarily constitute or imply its endorsement, recommendation, or favoring by the United States Government or any agency thereof, or the Regents of the University of California. The views and opinions of authors expressed herein do not necessarily state or reflect those of the United States Government or any agency thereof or the Regents of the University of California.

**EXPLORATORY TECHNOLOGY  
RESEARCH PROGRAM  
FOR  
ELECTROCHEMICAL ENERGY STORAGE**

**ANNUAL REPORT  
FOR 1991**

Energy & Environment Division  
Lawrence Berkeley Laboratory  
University of California  
Berkeley, California 94720

Edited by Kim Kinoshita, Technical Manager

June 1992

This work was supported by the Assistant Secretary for Conservation and Renewable Energy, Office of Propulsion Systems, Energy & Hybrid Propulsion Division of the U.S. Department of Energy under Contract No. DE-AC03-76SF00098.

# CONTENTS

<b>EXECUTIVE SUMMARY</b> .....	v
<b>I. INTRODUCTION</b> .....	1
<b>II. EXPLORATORY RESEARCH</b>	
<b>A. ADVANCED ZINC/NICKEL OXIDE CELLS</b>	
Zn/KOH/NiOOH Cell Studies .....	2
<b>B. SOLID-STATE SODIUM/POLYMER CELLS</b>	
Electrochemical Properties of Solid-State Sodium/Polymer Cells .....	3
<b>III. APPLIED SCIENCE RESEARCH</b>	
<b>A. ELECTRODE CHARACTERIZATION</b>	
Surface Morphology of Metals in Electrodeposition .....	5
Battery Materials: Structure and Characterization .....	7
<b>B. COMPONENTS FOR HIGH-TEMPERATURE CELLS</b>	
High-Temperature Cell Research .....	8
<b>C. CORROSION PROCESSES IN HIGH-SPECIFIC-ENERGY CELLS</b>	
Corrosion-Resistant Coatings for High-Temperature High-Sulfur-Activity Applications ....	9
Improved Container Electrode Coating for Na/S Battery Systems .....	10
Corrosion, Passivity, and Breakdown of Alloys Used in High-Energy Batteries .....	10
<b>D. COMPONENTS FOR AMBIENT-TEMPERATURE NONAQUEOUS CELLS</b>	
Spectroscopic Studies of the Passive Film on Alkali and Alkaline Earth Metals in	
Nonaqueous Solvents .....	12
<i>In Situ</i> Spectroscopic Applications to the Study of Rechargeable Lithium Batteries .....	14
Polymeric Electrolytes for Ambient-Temperature Batteries .....	16
Solid Polymer Electrolytes for Rechargeable Batteries .....	16
<i>In Situ</i> Raman Spectroscopy of Lithium Electrode Surfaces .....	17
<b>E. CROSS-CUTTING RESEARCH</b>	
Analysis and Simulation of Electrochemical Systems .....	18
Surface Layers on Battery Materials .....	19
Application of Photothermal Deflection Spectroscopy to Electrochemical Interfaces .....	20
Electrode Kinetics and Electrocatalysis of Methanol Electrooxidation .....	20
Effect of Electrocatalyst and Electrolyte Composition on Methanol/Air Fuel Cell	
Performance .....	22
<b>IV. AIR SYSTEMS RESEARCH</b>	
<b>A. METAL/AIR CELL RESEARCH</b>	
Electrocatalysts for Oxygen Electrodes .....	24
Novel Concepts for Oxygen Electrodes in Secondary Metal/Air Battery .....	26
Transport in Zinc-Air Cells and Mathematical Modeling .....	26
Development of Electrically Rechargeable Zinc/Air Cells .....	27
<b>B. FUEL CELL RESEARCH</b>	
Fuel Cells for Renewable Applications .....	28
Advanced Chemistry and Materials for Fuel Cells .....	33

## EXECUTIVE SUMMARY

The U.S. Department of Energy's Office of Propulsion Systems provides support for an electrochemical energy storage program, that includes research and development (R&D) on advanced rechargeable batteries and fuel cells. A major goal of this program is to develop electrochemical power sources suitable for application in electric vehicles (EVs). The program centers on advanced systems that offer the potential for high performance and low life-cycle costs, both of which are necessary to permit significant penetration into commercial markets.

The DOE Electrochemical Energy Storage Program is divided into two projects: the Electric Vehicle Advanced Battery Systems Development (EVABS) Program and the Exploratory Technology Research (ETR) Program. The EVABS Program management responsibility has been assigned to Sandia National Laboratory (SNL), and the Lawrence Berkeley Laboratory\* (LBL) is responsible for management of the ETR Program. The EVABS and ETR Programs include an integrated matrix of R&D efforts designed to advance progress on several candidate electrochemical systems. The United States Advanced Battery Consortium (USABC), a tripartite undertaking between DOE, the U.S. automobile manufacturers and the Electric Power Research Institute (EPRI), was formed in 1991 to accelerate the development of advanced batteries for consumer EVs. The role of the ETR Program is to perform supporting research on the advanced battery systems under development by the USABC and EVABS Program, and to evaluate new systems with potentially superior performance, durability and/or cost characteristics. The specific goal of the ETR Program is to identify the most promising electrochemical technologies and transfer them to the USABC, the battery industry and/or the EVABS Program for further development and scale-up. This report summarizes the research, financial and management activities relevant to the ETR Program in CY 1991. This is a continuing program, and reports for prior years have been published; they are listed at the end of the Executive Summary.

The general R&D areas addressed by the program include identification of new electrochemical couples for advanced batteries, determination of technical feasibility of the new couples, improvements in battery components and materials, establishment of engineering principles applicable to electrochemical energy storage and conversion, and the development of air-system (fuel cell, metal/air) technology for transportation applications. Major emphasis is given to applied research which will lead to superior performance and lower life-cycle costs.

---

\* Participants in the ETR Program include the following LBL scientists: E. Cairns, K. Kinoshita and F. McLarnon of the Energy and Environment Division; and L. DeJonghe, J. Evans, R. Muller, J. Newman, P. Ross and C. Tobias of the Materials Sciences Division.

The ETR Program is divided into three major program elements: Exploratory Research, Applied Science Research, and Air Systems Research. Highlights of each program element are summarized according to the appropriate battery system or electrochemical research area.

## EXPLORATORY RESEARCH

The objectives of this program element are to identify, evaluate and initiate development of new electrochemical couples with the potential to meet or exceed advanced battery and electrochemical performance goals. Research was conducted on new versions of the Zn/NiOOH cell, and a novel Na/polymer cell. Each of these cells is considered to be an attractive candidate for EV applications, and should provide high performance at ambient or near-ambient temperatures.

- LBL has demonstrated that the use of a moderately alkaline electrolyte is very effective for extending the cycle life of Zn/KOH/NiOOH cells. A 1.35-Ah sealed, starved-electrolyte cell containing 3.2 M KOH - 1.8 M KF - 1.8 M  $K_2CO_3$  retained 80% of its original charge after ~400 deep-discharge cycles and reached 570 cycles before its capacity fell below 60%. Scale up of Zn/KOH/NiOOH cells to 20 Ah (electrodes of  $\sim 15 \times 15$  cm) is underway, and the new electrolytes are being evaluated in these larger cells.
- LBL has initiated research to develop sodium/poly(ethylene) oxide/metal oxide electrode (Na/PEO/MO<sub>x</sub>) cells that operate at lower temperatures than typically used with Li/polymer cells. Preliminary half-cell experiments at 90°C with Na/PEO<sub>8</sub>CF<sub>3</sub>SO<sub>3</sub> demonstrated several cycles at either 0.25 or 0.5 mA/cm<sup>2</sup>. A metal oxide, Na<sub>0.6</sub>CoO<sub>2</sub>, for the cathode was synthesized in a single phase, and electrochemical testing is underway.

## APPLIED SCIENCE RESEARCH

The objectives of this program element are to provide and establish scientific and engineering principles applicable to batteries and electrochemical systems; and to identify, characterize and improve materials and components for use in batteries and electrochemical systems. Projects in this element provide research that supports a wide range of battery systems — alkaline, metal/air, flow, solid-electrolyte, and nonaqueous. Other cross-cutting research efforts are directed at improving the understanding of electrochemical engineering principles, minimizing corrosion of battery components, analyzing the surfaces of electrodes, and electrocatalysis.

**Alkaline Cells** often use Zn as the negative electrode, and it is this electrode that typically limits the lifetime of these cells. Efforts are underway to identify electrode and electrolyte compositions that will improve the cycle-life performance of the Zn electrode, and to determine the operating conditions that lead to dendrites and mossy deposits.

- LBL has completed a videomicroscopic study of the Zn deposition process from alkaline electrolytes in a flow channel. Decreasing the zincate ion and increasing the OH<sup>-</sup> ion concentrations promote the growth of Zn moss. At constant fraction of limiting current, the moss appears more readily when the current density and/or the flow rate is low.
- Brookhaven National Laboratory (BNL) has used extended x-ray absorption fine structure (EXAFS) and x-ray absorption near-edge spectroscopy (XANES) to study mossy Zn deposits that form in alkaline zincate electrolytes. The Zn that deposits at -65 mV (*vs* Zn wire reference electrode) is oriented with the c-axis parallel to the lines of current, whereas the deposit at -45 mV has a random orientation like that of a Zn foil.

**Improved Components for Alkali/Sulfur Cells**, such as superior alternatives to the high-temperature sulfur-polysulfide electrode for Na/S cells, are under investigation.

- LBL is investigating the influence of phosphorus on the sulfur electrode of the Na/S cell by equilibrium open-circuit potential measurements. Mixtures with P/S molar ratios from 0.143 to 0.60 and Na mole fractions from 0.0 to 0.4 were studied at 350 and 400°C. The Na/P<sub>x</sub>S<sub>y</sub> cells showed significantly higher cell voltages than Na/S cells, which is a strong indication that phosphorus may be a beneficial additive to the sulfur electrode.

**Corrosion Processes in High-Specific-Energy Cells** are under investigation and the aim is to develop low-cost container and current-collector materials for use in nonaqueous, alkali/sulfur, and molten-salt cells.

- Illinois Institute of Technology (IIT) is optimizing the quality of electrodeposited Mo<sub>2</sub>C coatings to obtain long-term endurance in Na/S cells. IIT observed that complete removal of moisture from the electrolysis bath is necessary to obtain a reproducible, high quality coating. Coatings of an even better quality were obtained with a bath containing non-Li alkali molybdates and carbonates.
- A new project was initiated at Environmental Research Institute of Michigan (ERIM) to evaluate TiN-coated containment materials in Na/S cells. Preliminary studies at Ford Motor Company indicated that sputter-coated TiN on Al was resistant to attack in a polysulfide melt during the 72-h test. A reactive-sputtering system is being assembled at ERIM to dupli-

cate the quality of the coatings obtained at Ford, and to evaluate the corrosion-resistant properties of TiN for extended periods in polysulfide melts.

- Johns Hopkins University has observed that iron and 1018 carbon steel display an extensive and stable passive region in LiAsF<sub>6</sub>/dimethoxyethane (DME). In a nominally dry LiAsF<sub>6</sub>/DME solution (<100-ppm H<sub>2</sub>O), the breakdown potentials of iron and carbon steel are 1300 mV (*vs* saturated calomel electrode, SCE) and 1050 mV, respectively. The adsorption of DME and the formation of carbon-based polymer film are believed to be responsible for passivation.

**Components for Ambient-Temperature Nonaqueous Cells**, particularly metal/electrolyte combinations that improve the rechargeability of these cells, are under investigation.

- Case Western Reserve University (CWRU) has used *in situ* spectroscopic techniques and thermal analysis to study the Li/organic electrolyte and Li/poly(ethyleneoxide) interfaces. Interactions between Li and tetrahydrofuran, and the formation of Li-O and Li-CO<sub>3</sub> species, were detected. A new project was initiated in 1991 at CWRU to place greater emphasis on the investigation of the Li/polymer interface. Preliminary cyclic voltammetry studies of Au in contact with LiClO<sub>4</sub>- poly(ethylene oxide) electrolyte at 55°C showed evidence for underpotential deposition (UPD) of Li.
- The University of Pennsylvania has investigated polymeric electrolytes formed by radiation-polymerization of various oligomers that contain different compositions of plasticizer (ethylene carbonate, EC, and propylene carbonate, PC) and 1 M LiAsF<sub>6</sub>. Polymeric electrolytes with ≥50 wt% PC in mixtures with EC appear to exhibit acceptable electrochemical (reversible Li redox process) and physicochemical properties (ionic conductivity >8 × 10<sup>-4</sup> at room temperature, glass-transition temperature of -94°C, amorphous structure from -90 to 150°C) for use in rechargeable Li cells.
- SRI International has developed a Li-ion conducting PEO-type polymer in which oxygen is replaced by sulfur. The best-performing polymer electrolyte, obtained from sulfur-substituted PEO (16.7% S) and tetraethylorthosilicate with a plasticizer, exhibited a conductivity of 7.5 × 10<sup>-4</sup> ohm<sup>-1</sup> cm<sup>-1</sup> in a Li/Li cell.
- Jackson State University has evaluated the electrochemical properties of the C<sub>60</sub> fullerene as an electrode material that may be useful in rechargeable Li cells. The cyclic voltammograms of C<sub>60</sub> in LiClO<sub>4</sub>/polyethylene glycol 400 dimethyl ether (PEG400DME) indicated five redox peaks which suggested the formation of C<sub>60</sub><sup>-</sup>, C<sub>60</sub><sup>2-</sup>, C<sub>60</sub><sup>3-</sup>, C<sub>60</sub><sup>4-</sup>, and C<sub>60</sub><sup>5-</sup>. These anions dissolve in PEG400DME.

**Cross-Cutting Research** is carried out to develop mathematical models of electrochemical systems and to address fundamental problems in electrocatalysis and current-density distribution; solutions will lead to improved electrode structures and performance in batteries and fuel cells.

- LBL has developed mathematical models to understand transport and kinetic phenomena occurring in electrochemical systems. Improvements to the model of a solid-polymer-electrolyte (SPE) fuel cell were made to include the effects of electrode kinetics, mass transfer to the membrane-electrode interface, and thermal effects. Models were also developed for explaining electroless deposition and cathodic protection.
- LBL has observed by scanning tunneling microscopy (STM) that the transformation of nickel hydroxide to oxy-hydroxide during the charging of Ni electrodes in alkaline solution proceeds by nucleation and growth of the oxidized phase from the metal surface. Model calculations have shown that, because of the much higher conductivity of the oxidized material versus reduced material, the reaction front for the conversion propagates in a nonuniform fashion, leaving large amounts of unreacted material behind.
- LBL is using photothermal deflection spectroscopy (PDS) to study the electrooxidation of  $\text{CH}_3\text{OH}$  on Pt electrocatalyst. This study indicates that the rate-limiting step appears to be the transfer of oxygen from water to the Pt catalyst where it can react with  $\text{CH}_3\text{OH}$  to form  $\text{CO}_2$ . PDS is also being developed for the *in situ* detection of adsorbed intermediates during the electrooxidation of organic molecules on Cu. A Xe arc lamp is being used to obtain UV-visible absorption spectra of reduced intermediates that form during the electrocatalytic hydrogenation of nitrobenzene on Cu.
- LBL has observed that the surface composition of Pt ( $\text{MPt}_3$ ) alloys for methanol electrooxidation is strongly dependent on the strength of the intermetallic Pt-M bond. In  $\text{CoPt}_3$ , for example, where the intermetallic bond is relatively weak, the lower surface energy of Pt produced pure Pt planes on both the [111] and [100] orientation.
- LBL confirmed that dispersed Pt-Ru has a much higher catalytic activity for the electrooxidation of vaporized methanol than Pt alone in 72 wt%  $\text{Cs}_2\text{CO}_3$  at 120°C. Furthermore, a cell with 72 wt%  $\text{Cs}_2\text{CO}_3$  exhibited much lower potential losses than a comparable cell operated with concentrated  $\text{H}_3\text{PO}_4$  under similar conditions (80°C).

## AIR SYSTEMS RESEARCH

The objectives of this program element are to identify, characterize and improve materials for air electrodes; and to identify, evaluate and initiate development of metal/air battery systems and fuel-cell technology for transportation applications.

**Metal/Air Cell Research** projects address bifunctional air electrodes, that are needed for electrically rechargeable metal/air (Zn/air, Fe/air) cells; and novel alkaline Zn electrode structures, that could be used in either electrically recharged or mechanically recharged cell configurations.

- CWRU has observed that the catalytic activity for the reduction of  $O_2$  at cobalt tetrasulfonated phthalocyanine (CoTsPc) adsorbed on ordinary pyrolytic graphite (OPG) in alkaline solution is enhanced by ~60 mV in the presence of alcohols. Further, the presence of methanol has no short-term deleterious effect on the kinetics for  $O_2$  reduction on CoTsPc/OPG, which also exhibits negligible catalytic activity for methanol oxidation.
- A program was initiated at Eltech Research Corporation to investigate the viability of graphitized carbon blacks and metal oxides as electrocatalyst supports in bifunctional air electrodes for electrically rechargeable Zn/air cells. Graphitized carbon blacks of Monarch 120 and Shawinigan acetylene black, and the metal oxides of  $NiCo_2O_4$ ,  $Co_3O_4$ ,  $Pb_2Ru_2O_7$  and  $Pb_2Ir_2O_7$ , have been prepared. Electrochemical tests will be underway shortly in small cells at Metal Air Technology Systems International (MATSI).
- LBL has initiated experiments to adapt the mechanically rechargeable Zn/air cell invented at LBL, which employed a reticulated Zn electrode structure to operate under natural convection, for electrically rechargeable cell configurations. A laser-Doppler velocimeter has been modified to measure the electrolyte velocity, and the expected signal was obtained. An algorithm has been developed to model the convective diffusion of the electrolyte in the porous electrode structure.
- LBL is evaluating commercial bifunctional air electrodes in Zn/air cells, as well as developing improved bifunctional air electrodes from metal oxide electrocatalysts. A bifunctional air electrode (BF-8) from Electromedia, Inc. was evaluated at constant-current rates and the Simplified Federal Urban Driving Schedule (SFUDS) in a Zn/air cell with an electrolyte of 45 wt% KOH and 40 g  $Zn^{2+}$ /l. Approximately 25 cycles were achieved, regardless of the discharge rates.

**Fuel Cell Research** at Los Alamos National Laboratory (LANL) includes research in several areas of electrochemistry, theoretical studies, fuel-cell testing, fuel processing, and membrane characterization. Major achievements of the fuel-cell program during 1991 are listed below:

- LANL has found that processing membrane-electrode assemblies (MEA) with membranes that contain the  $\text{Na}^+$  form rather than the  $\text{H}^+$  form permits the use of higher processing temperatures, 185 vs 135°C. The MEA are more robust, have a lower impedance, and are more tolerant to adverse humidification conditions in fuel cells.
- LANL has characterized some of the  $\text{H}_2\text{O}$ -management properties of Nafion 117, membrane C, and an experimental Dow membrane. The Dow membrane appears to show the highest  $\text{H}_2\text{O}$  uptake and smallest water drag. These properties are beneficial for obtaining high performance in fuel cells with the Dow membrane.
- LANL has resolved the problem of membrane puncture that was observed in small fuel cells that contain thin membranes such as the 2-mil thick Nafion membrane. The problem was overcome by using a thin Teflon gasket in the membrane/electrode/gasket assembly to prevent the sensitive area of the membrane from direct exposure to the reactant gases.
- A large 50-cm<sup>2</sup> cell was operated at LANL which attained an initial performance of 2 A/cm<sup>2</sup> on  $\text{O}_2$  (5 atm) without experiencing transport losses at the  $\text{O}_2$  electrode. The initial performance on air (5 atm) showed only marginal losses up to 1 A/cm<sup>2</sup>.
- It is concluded from the one-dimensional model developed by LANL that the counter fluxes of  $\text{H}^+$  and  $\text{O}_2$  in the fuel cell determine the degree of utilization of the catalyst layer along its thickness direction.
- Polymer membranes were synthesized at LANL from Nafion and siloxane monomers that are significantly stiffer than Nafion, and also exhibit a low tendency to take up methanol. These membranes may be effective in lowering the methanol solubility in fuel cells with polymer membranes.
- BNL is utilizing x-ray absorption spectroscopy (XAS) to investigate the properties of Pt/C and several of its alloys with Cr, Co, and Ni. The results indicate that alloying with Ni has a large effect on the d character of Pt, whereas Cr has little effect. Nickel forms a solid solution with Pt, with the Ni atoms substituting at Pt sites.

## MILESTONES FOR THE EXPLORATORY TECHNOLOGY RESEARCH PROGRAM

Milestones accomplished in Fiscal Year 1991 by the ETR Program include:

- "Demonstrate high performance of new structures of the membrane-electrode assembly in polymer electrolyte fuel cells (PEFC) with Pt loadings  $\leq 0.2 \text{ mg/cm}^2$ "

The LANL test showed that the performance of a single cell with  $\leq 0.175 \text{ mg/cm}^2$  Pt + 50-nm sputtered Pt is comparable to that obtained with  $\leq 0.45 \text{ mg/cm}^2$  Pt loading.

- "Complete one-dimensional model for PEFC based on experimentally derived transport parameters"

The LANL model employs experimentally measured parameters such as water diffusion coefficient, electroosmotic drag coefficients, water sorption isotherms, and membrane conductivities. The model predicts a net-water-per-proton flux ratio of  $0.2 \text{ H}_2\text{O}/\text{H}^+$  under typical operating conditions, which is much less than the measured electroosmotic drag coefficient for a fully hydrated Nafion 117 membrane.

- "Begin Zn/air cell development activities with the EVABS Program"

LBL and SNL have completed a joint program plan entitled "Program Plan for Development of Zinc/Air Batteries," which was submitted to DOE/HQ on May 2, 1991. In addition, we have provided our input to the Statement-of-Work for the Request for Quotations (RFQ) from SNL on "Development of a Metal/Air Battery for Electric Vehicles Applications." These activities are intended to provide a smooth transition for the Zn/air battery program as the emphasis of the program shifts from research at LBL to engineering development at SNL. It is anticipated that LBL will continue to work closely with SNL in the future by assisting with the evaluation of the responses to the RFQ, serving at program review meetings, and coordinating its research projects to support the battery development effort.

- "Go/no-go decision to continue investigations on molten-salt electrodeposition and chemical-vapor deposition (CVD) as methods to produce corrosion-resistant coatings for high-temperature batteries"

A renewal proposal was submitted by IIT to continue their studies on the use of molten-salt deposition and CVD to produce corrosion-resistant coatings. Based on the reviewers' comments and the evaluation by the ETR Program Selection Committee, it is recommended that the project should continue for another year. IIT was encouraged to transfer their technology to an industrial company.

- "Complete *ex situ* EXAFS studies of PbO<sub>2</sub>"

A combination of XANES and EXAFS was used to determine the coordination number, symmetry and bond lengths for Pb<sup>2+</sup> ions in aqueous solutions and Pb<sup>4+</sup> ions in glacial acetic acid. Studies were also made on the two polymorphs of PbO and PbO<sub>2</sub>. Features of the XANES spectra were interpreted in terms of hybridized orbitals, multiple scattering effects, and crystal-field splitting of d orbitals. All the Pb(IV) materials displayed a pre-edge feature due to 2p → 6s transitions. In the case of PbO<sub>2</sub> the intensity of this transition was correlated with the stoichiometry of the oxide. There were clear differences in the radial structure functions for α-PbO<sub>2</sub> and β-PbO<sub>2</sub> due to focusing effects in the latter. These peaks at large R values are a clear signature for fingerprinting the β-PbO<sub>2</sub> phase.

- "Complete EXAFS studies of adatom-modified Pt catalysts"

Underpotential deposited (UPD) Cu on Pt-supported-on-carbon electrocatalyst was investigated *in situ* in 0.5 M H<sub>2</sub>SO<sub>4</sub> at 0.05 V (*vs* SCE) by XANES. By taking XANES spectra at the Cu K-edge and the Pt L<sub>111</sub>-edge, it was possible to determine the valence state of Cu and observe modifications in the electronic structure of the Pt with adsorbed Cu. The XANES for UPD Cu shows that the adsorbed Cu has an oxidation state close to that of Cu<sup>+</sup>. XANES features strongly indicate a tetrahedral coordination for the adsorbed Cu species. A reduction in intensity of the white line in the Pt XANES is consistent with a partial filling of empty Pt d-band vacancies by adsorption of Cu. Thus, UPD species can modify the electronic structure of Pt catalysts. The adsorbed Cu<sup>+</sup> species are apparently associated with HSO<sub>4</sub><sup>-</sup> ions.

- "Initiate new research project on novel processing techniques to improve the surface properties of metals, alloys and seal components for batteries"

In March 1991, LBL published a notice in Commerce Business Daily to solicit research on novel surface processing techniques that could benefit batteries for EVs. Six proposals were received in response to our Request for Proposals (RFP), and they were reviewed by LBL and outside technical experts. On the basis of these reviews and other considerations such as qualifications, facilities, program management, business aspects, *etc.*, a subcontract was awarded to the Environmental Research Institute of Michigan (ERIM). The principal investigator is Dr. Thomas K. Hunt, who previously worked at Ford Motor Company on the sodium heat engine. The goal of the research project is to develop thin coatings of TiN to protect the surface of cell components for Na/S cells. The corrosion-resistant properties of TiN coatings which are sputter-deposited on Al substrates will be investigated under a variety of electrochemical conditions appropriate for Na/S battery operation.

## MANAGEMENT ACTIVITIES

During 1991, LBL managed 15 subcontracts and conducted a vigorous research program in electrochemical energy storage. LBL staff members attended project review meetings, made site visits to subcontractors, and participated in technical management of various ETR projects. LBL staff members also participated in the following reviews, meetings, and workshops:

- FY 1993 DOE/CRE Program Planning Workshop, SERI, February 20-22, 1991
- Lithium-Ion Battery Meeting, SNL, February 22, 1991
- U.S. Advanced Battery Consortium Meeting, Highland Park, MI, April 19, 1991
- 179th Meeting of the Electrochemical Society, Washington, D.C., May 5-10, 1991
- IAPG Meeting, Albuquerque, NM, May 20, 1991
- 4th World Congress of Chemical Engineering, Karlsruhe, Germany, June 15-19, 1991
- 26th IECEC, Boston, MA, August 4-9, 1991
- 42nd Meeting of the International Society of Electrochemistry, Montreux, Switzerland, August 25-28, 1991
- LANL Fuel Cell Review Meeting, Washington, D.C., August 28, 1991
- U.S. Advanced Battery Consortium Meeting, LBL, Berkeley, CA, September 20, 1991
- 180th Meeting of the Electrochemical Society, Phoenix, AZ, October 13-17, 1991
- U.S. Advanced Battery Consortium Meeting, SNL, Albuquerque, NM, October 18, 1991
- Quarterly Project Review of Zn/NiOOH System, EPRI, Palo Alto, CA, October 22, 1991
- Annual Automotive Technology Development Contractors' Coordination Meeting, Dearborn, MI, October 28-31, 1991
- Workshop on Structural Effects in Electrocatalysis and Oxygen Electrochemistry, Cleveland, OH, October 29-November 1, 1991
- Workshop on DOE Carbon Foam Materials, SNL, Livermore, CA, November 6, 1991

## ACKNOWLEDGMENT

This work was supported by the Assistant Secretary for Conservation and Renewable Energy, Office of Propulsion Systems, Energy & Hybrid Propulsion Division of the U.S. Department of Energy under Contract No. DE-AC03-76SF00098. The support from DOE and the contributions by the participants in the ETR Program are acknowledged. The assistance of Ms. Susan Lauer for coordinating the publication of this report and Mr. Garth Burns for providing the financial data are gratefully acknowledged.

## ANNUAL REPORTS

1. "Technology Base Research Project for Electrochemical Energy Storage - Annual Report for 1990," LBL-30846 (June 1991).
2. "Technology Base Research Project for Electrochemical Energy Storage - Annual Report for 1989," LBL-29155 (May 1990).
3. "Technology Base Research Project for Electrochemical Energy Storage - Annual Report for 1988," LBL-27037 (May 1989).
4. "Technology Base Research Project for Electrochemical Energy Storage - Annual Report for 1987," LBL-25507 (July 1988).
5. "Technology Base Research Project for Electrochemical Energy Storage - Annual Report for 1986," LBL-23495 (July 1987).
6. "Technology Base Research Project for Electrochemical Energy Storage - Annual Report for 1985," LBL-21342 (July 1986).
7. "Technology Base Research Project for Electrochemical Energy Storage - Annual Report for 1984," LBL-19545 (May 1985).
8. "Annual Report for 1983 - Technology Base Research Project for Electrochemical Energy Storage," LBL-17742 (May 1984).
9. "Technology Base Research Project for Electrochemical Energy Storage - Report for 1982" LBL-15992 (May 1983).
10. "Technology Base Research Project for Electrochemical Energy Storage - Report for 1981," LBL-14305 (June 1982).
11. "Applied Battery and Electrochemical Research Program Report for 1981," LBL-14304 (June 1982).
12. "Applied Battery and Electrochemical Research Program Report for Fiscal Year 1980," LBL-12514 (April 1981).

## LIST OF ACRONYMS

AES	Auger electron spectroscopy
AFM	atomic force microscopy
BNL	Brookhaven National Laboratory
CMD	chemical manganese dioxide
CVD	chemical vapor deposition
CWRU	Case Western Reserve University
DC	direct current
DEC	diethyl carbonate
DMC	dimethyl carbonate
DME	dimethoxyethane
DMFC	direct methanol fuel cell
DOE	Department of Energy
DSC	differential scanning calorimetry
EC	ethylene carbonate
EMD	electrolytic manganese dioxide
EPRI	Electric Power Research Institute
ERIM	Environmental Research Institute of Michigan
ETR	Exploratory Technology Research
EV	electric vehicle
EVABS	Electric Vehicle Advanced Battery Systems
EW	equivalent weight
EXAFS	extended x-ray absorption fine structure
FTIRRAS	Fourier transform infrared reflectance absorption spectroscopy
GDL	gas diffusion layer
HOPG	highly ordered pyrolytic graphite
IECEC	Intersociety Energy Conversion Engineering Conference
IIT	Illinois Institute of Technology
ISE	International Society of Electrochemistry
LANL	Los Alamos National Laboratory
LBL	Lawrence Berkeley Laboratory
LEED	low energy electron diffraction
MEA	membrane electrode assemblies
MATSI	Metal Air Technology Systems International
MF	methyl formate

MSECD	molten salt electrochemical deposition
NMR	nuclear magnetic resonance
OCP	open circuit potential
OPG	ordinary pyrolytic graphite
PC	propylene carbonate
PDS	photothermal deflection spectroscopy
PECVD	plasma-enhanced chemical vapor deposition
PEM	proton-exchange membrane
PEO	poly(ethylene oxide)
PPO	poly(propylene oxide)
PTFE	polytetrafluoroethylene
pzc	point of zero charge
QCM	quartz crystal microbalance
RDE	rotating disk electrode
RFP	Request for Proposal
RFQ	Request for Quotations
RL	reaction layer
SCE	saturated calomel electrode
SEM	scanning electron microscopy
SERS	surface-enhanced Raman spectroscopy
SFUDS	Simplified Federal Urban Driving Schedule
SNL	Sandia National Laboratories
SPE	solid polymer electrolyte
STM	scanning tunneling microscopy
TEM	transmission electron microscopy
TEOS	tetraethylorthosilicate
TGA	thermogravimetric analysis
THF	tetrahydrofuran
TMPP	tetramethoxyphenyl porphyrin
TPD	temperature programmed desorption
UHV	ultrahigh vacuum
UPD	underpotential deposition
USABC	United States Advanced Battery Consortium
XANES	x-ray near edge absorption spectroscopy
XAS	x-ray absorption spectroscopy
XPS	x-ray photoelectron spectroscopy

# SUBCONTRACTOR FINANCIAL DATA - CY 1991

Subcontractor	Principal Investigator	Project	Contract Value (K\$)	Term (months)	Expiration Date	Status in CY 1991*
<b><u>APPLIED SCIENCE RESEARCH</u></b>						
Lawrence Berkeley Laboratory	E. Cairns, L. DeJonghe, J. Evans, R. Muller, J. Newman, P. Ross, and C. Tobias	Electrochemical Energy Storage	1800	12	9-91	C
<b>Acid Cells</b>						
Brookhaven National Laboratory	J. McBreen	Battery Materials	100	12	9-91	C
<b>Components for High-Temperature Cells</b>						
Stanford University	R. Huggins	New Battery Materials	78	6	4-92	T
<b>Corrosion Processes in High-Specific Energy Cells</b>						
Illinois Institute of Technology	R. Selman	Corrosion Resistant	132	12	8-92	T
Environmental Research Institute of Michigan	T. Hunt	Secondary Batteries	105	12	8-92	C
Johns Hopkins University	J. Kruger	Corrosion/Passivity Studies	30	12	8-92	T
<b>Components for Ambient-Temperature Nonaqueous Cells</b>						
Case Western Reserve University	D. Scherson	Spectroscopic Studies	55	12	4-92	T
Case Western Reserve University	D. Scherson	<i>In Situ</i> Studies	86	12	7-92	C
Jackson State University	H. Tachikawa	Raman Spectroscopy	47	23	5-92	T
University of Pennsylvania	G. Farrington	Polymeric Electrolytes	50	12	7-92	T
SRI International	S. Narang	Polymeric Electrolytes	97	12	9-91	T
<b><u>AIR SYSTEMS RESEARCH</u></b>						
<b>Metal/Air Cell Research</b>						
Eltech Research Corporation	E. Rudd	Oxygen Electrodes	125	13	8-92	T
Case Western Reserve University	E. Yeager	Air Electrodes	150	12	4-92	T
Metal Air Technology Systems	R. Putt	Zn/Air Battery	50	5	5-91	T
<b>Fuel Cell R&amp;D</b>						
Los Alamos National Laboratory	S. Gottesfeld	Fuel Cell R&D	1400	12	9-91	C
Brookhaven National Laboratory	J. McBreen	Fuel Cell Research	100	12	9-91	C

\* C = continuing, T = terminating

# I. INTRODUCTION

This report summarizes the progress made by the Exploratory Technology Research (ETR) Program for Electrochemical Energy Storage during calendar year 1991. The primary objective of the ETR Program, which is sponsored by the U.S. Department of Energy (DOE) and managed by Lawrence Berkeley Laboratory (LBL), is to identify electrochemical technologies that can satisfy stringent performance, durability and economic requirements for electric vehicles (EVs). The ultimate goal is to transfer the most-promising electrochemical technologies to the private sector or to another DOE program (e.g., SNL's Electric Vehicle Advanced Battery Systems Development Program, EVABS) for further development and scale-up.

Besides LBL, which has overall responsibility for the ETR Program, LANL and BNL have participated

in the ETR Program by providing key research support in several of the program elements.

The ETR Program consists of three major elements:

- Exploratory Research
- Applied Science Research
- Air Systems Research

The objectives and the specific battery and electrochemical systems addressed by each program element are discussed in the following sections, which also include technical summaries that relate to the individual programs. Financial information that relates to the various programs and a description of the management activities for the ETR Program are described in the Executive Summary.

## II. EXPLORATORY RESEARCH

The major thrust of this program element is to evaluate promising electrochemical couples for advanced batteries for electric vehicles (EVs). Exploratory research was carried out on Zn/NiOOH and Na/metal oxide polymerization cells. Novel components for various versions of rechargeable Li, Na, and Zn cells were also investigated, as described in the Applied Science section of this report.

### A. ADVANCED ZINC/NICKEL OXIDE CELLS

New approaches to extend the cycle life of Zn/NiOOH cells are underway that involve modifying the electrolyte composition.

#### Zn/KOH/NiOOH Cell Studies

*E.J. Cairns and F.R. McLarnon (Lawrence Berkeley Laboratory)*

This research studies the life- and performance-limiting phenomena of Zn/NiOOH cells under realistic operating conditions. The use of moderately alkaline electrolytes\* has proven to be a very effective means for extending the cycle life of the Zn/NiOOH cell. Reducing the electrolyte concentration from ~30 to ~15 wt% KOH reduces the Zn species solubility by a factor of four, thereby significantly slowing the rate of Zn redistribution (shape change) and increasing the cell cycle life by a factor of five.

A 1.35-Ah sealed, starved-electrolyte cell containing 3.2 M KOH - 1.8 M KF - 1.8 M K<sub>2</sub>CO<sub>3</sub> electrolyte retained 80% of its original capacity after ~400 deep-discharge cycles and reached 570 cycles before its capacity fell below 60%. Oxygen produced at the NiOOH electrode near the end of cell charging quickly reached a steady-state absolute pressure of 1.0-1.5 bar. The efficient recombination of O<sub>2</sub> with Zn preserved the balance between reduced and oxidized forms of Zn. Also no dendritic growths or cell shorts occurred at any time during the cell lifetime, therefore the cell was maintenance-free.

\* LBL has submitted a U.S. patent application covering the use of these superior electrolytes and is actively promoting the transfer of this new technology to industry.

*In situ* x-ray photographs were recorded at periodic intervals throughout the life of the cell revealing a stable Zn morphology with remarkably little shape change. The performance of this and other moderately alkaline cells was consistently limited by the NiOOH electrode, therefore further extensions of cycle life will require the optimization of NiOOH electrodes for use in these cells. The Zn/NiOOH cell is environmentally benign, compared to the Cd/NiOOH cell, and could be an attractive candidate for rechargeable battery applications.

A 20-Ah Zn/NiOOH cell with large electrodes, ~15 × 15 cm, suitable for use in EV-size Zn/NiOOH batteries, is under development. Most of the scale-up problems have been solved, including the design and fabrication of large, uniform Zn electrodes and large air-tight cell cases. Significant accumulation with excessive pressures was a problem in the first large sealed cells tested. Placement of a small piece of supported Pt catalyst material within the cell eliminated the H<sub>2</sub> by rapidly combining it with O<sub>2</sub> released by NiOOH electrodes during charge. The remaining O<sub>2</sub> readily combined with Zn yielding a steady-state pressure below 1 bar. A 15-Ah "baseline" cell containing 31 wt% KOH electrolyte achieved 140 cycles, which is comparable to the performance of 1.35-Ah sealed cells and confirms that the scale-up to larger cell sizes has been successful. The superior alkaline-fluoride-carbonate electrolyte is now being evaluated in a sealed 20-Ah cell.

Work is near completion on a new 486-based PC system for cycling cells. Special power supplies, current controllers and signal amplifiers have been built and tested. Control software for the system has been developed using the "LT/Control" platform provided by Labtech, Inc. in an OS/2 multitasking environment, thereby allowing each cell to be managed independently by its own virtual CPU. This new system will provide larger currents and greater versatility for testing the power and lifetime characteristics of electrochemical cells.

#### PUBLICATIONS

1. J. Weaver, F.R. McLarnon, and E.J. Cairns, "Experimental and Theoretical Study of Concentration Distributions in a Model Pore Electrode. I. Measurement of Two-Dimensional Concentration Gradients in a Zinc Model Pore, *J. Electrochem. Soc.*, **138**, 2572 (1991).

2. J. Weaver, F.R. McLarnon, and E.J. Cairns, "Experimental and Theoretical Study of Concentration Distributions in a Model Pore Electrode. II. Mathematical Models and Comparison to Experiment, *J. Electrochem. Soc.*, **138**, 2579-85 (1991).
3. T.C. Adler, F.R. McLarnon, and E.J. Cairns, "Rechargeable Zinc Cell with Alkaline Electrolyte Which Inhibits Shape Change in Zinc Electrode," U.S. Patent Application (1991).

## B. SOLID-STATE SODIUM/POLYMER CELLS

Efforts are underway to develop all-solid-state Na/polymer cells. The studies focus on demonstrating the viability of a sodium/sodium-alloy negative and a metal oxide positive in a rechargeable cell with a polymeric electrolyte.

### Electrochemical Properties of Solid-State Sodium/Polymer Cells

*L.C. DeJonghe (Lawrence Berkeley Laboratory)*

Research is underway to develop all-solid-state cells based on a sodium/sodium-alloy negative electrode, polymeric electrolytes, and a metal oxide positive electrode (Na/PEO/MO<sub>x</sub>). Sodium or sodium alloy electrodes are attractive for use in solid polymer cells because of the low cost and wide availability of bulk Na, and its ease of fabrication and malleability. The ionic conductivity of poly(ethylene oxide) (PEO) complexed with Na salts is as high or higher than the corresponding Li salts, which should be beneficial for Na/PEO/MO<sub>x</sub> cells. A number of studies have reported a transport number of 0.5 or lower for Li transport in PEO, but few studies have been conducted on Na transport. It is possible that the lower affinity of Na<sup>+</sup> for ethereal oxygen in PEO translates to a higher transport number for Na relative to Li in PEO. In this case, the actual cationic conductivity of PEO would be significantly higher for Na salts than for Li salts.

Studies with Na and Na-alloy negative electrodes and sodium cobalt bronze positive electrodes immersed in nonaqueous solvents have shown good rate capability (1-2 mA/cm<sup>2</sup>), high, ~3.5 V, open circuit voltage (OCV) and very reversible cycling; 300 cycles were attained with 1000 cycles projected. The use of solid polymer electrolytes (SPEs) should improve the characteristics of the Na/electrolyte interface, as well as dramatically increase the system safety. Further-

more, if the intercalation of Na into petroleum coke is sufficiently reversible and kinetically facile, it may be possible to fabricate Na-ion rocking chair cells in a manner analogous to recent developments in Li-ion technology.

Half cells consisting of Na electrodes and (PEO)<sub>8</sub>NaCF<sub>3</sub>SO<sub>3</sub> were successfully cycled at 90°C for several cycles at either 0.25 or 0.5 mA/cm<sup>2</sup>. Figure 1 shows the voltage transients during constant-current discharge (with periodical excursions to open circuit) at 0.5 mA/cm<sup>2</sup> of a Na/PEO/Na cell. Although there was some instability in the first cycle, the voltage stabilized subsequently. This may be interpreted to mean that Na initially reacts with PEO to form a conductive and protective interface layer. This is analogous to the behavior seen in Li cells with liquid or polymer electrolytes. The Na cells had a tendency to short after several cycles. Because the melting point of Na is 97°C, and the optimum temperature for operation of SPE cells is 90°C, the likelihood of local melting of Na, resulting in internal shorting, is great. For this reason, it may be more fruitful to substitute Na-3.5 Pb alloy or Na/C for Na in intermediate-temperature Na/PEO cells. Another approach is to use Na metal in room-temperature cells containing amorphous PEO as the polymer electrolyte. Amorphous PEO has been used successfully with Li in room-temperature, SPE cells in this laboratory, but little is known about its behavior with Na.

Cells consisting of Li anodes and petroleum coke cathodes with liquid electrolytes were assembled and cycled as models for the Na/C system. Successful cycling to LiC<sub>12</sub> was accomplished at the C/30 rate.

Appropriate cathode materials for Na/PEO-based cells must be identified. Although less work has been done in this area as compared to Li intercalation, a number of promising metal oxides have been reported in the literature. The most promising candidates are V<sub>6</sub>O<sub>13</sub>, amorphous V<sub>2</sub>O<sub>5</sub>, Na<sub>x</sub>MnO<sub>2</sub>, Na<sub>x</sub>CoO<sub>2</sub>, Na<sub>x</sub>NiO<sub>2</sub>, and Na<sub>x</sub>CrO<sub>2</sub>. The sodium cobalt bronze, Na<sub>0.6</sub>CoO<sub>2</sub>, in the P2 phase was synthesized by reacting Co<sub>3</sub>O<sub>4</sub> with Na<sub>2</sub>CO<sub>3</sub> in the solid state under oxygen at 750°C for 27 h. X-ray diffraction analysis indicated that the reaction was complete and a single phase was produced. Several different phases of sodium cobalt bronzes may be synthesized readily by varying the amount of Na salt and the reaction conditions. Many of these phases have been discharged successfully in Na cells with liquid electrolytes; however, the P2 form shows the widest range of electrochemical Na intercalation and de-intercalation (from 0 to 0.7 Na per Co) without phase change and therefore has the best cyclability.

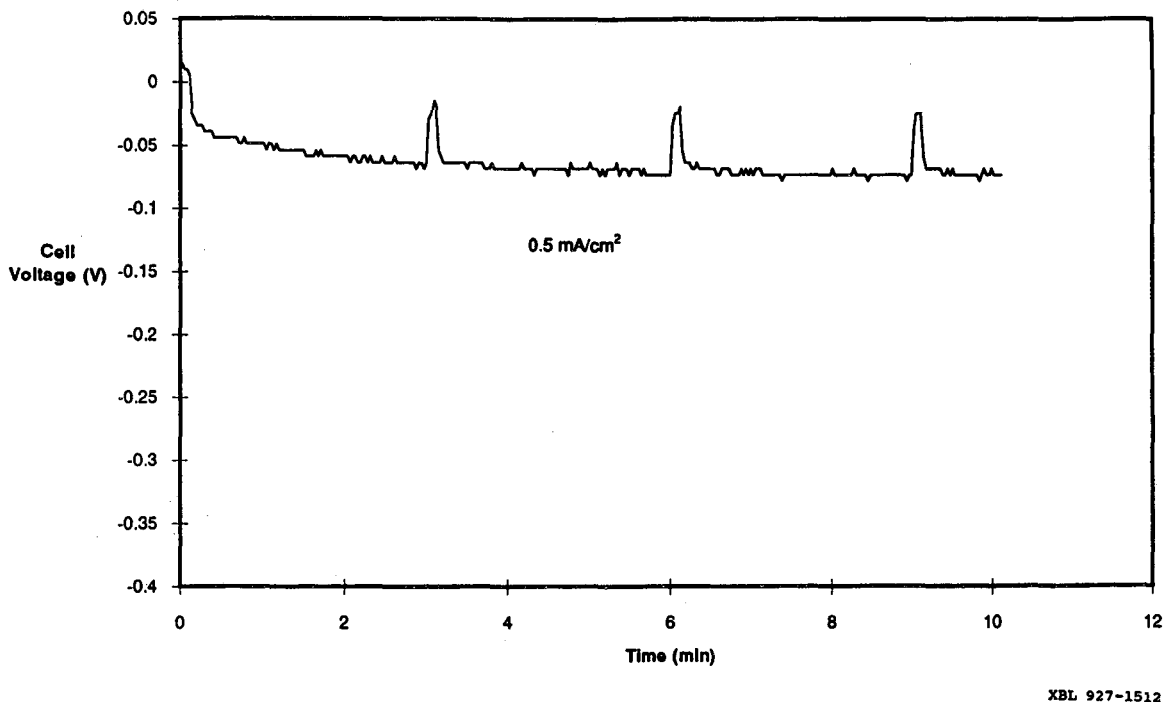


Figure 1. Discharge of Na/PEO-NaTf/Na cell at 0.5 mA/cm<sup>2</sup>.

#### PUBLICATIONS

1. M. Liu, S.J. Visco, and L.C. De Jonghe, "Novel Solid Redox Polymerization Electrodes: Electrochemical Properties," *J. Electrochem. Soc.*, **138**, 1896 (1991).
2. M. Liu, S.J. Visco, and L.C. De Jonghe, "Novel Solid Redox Polymerization Electrodes: All-Solid-State, Thin-Film, Rechargeable Lithium Batteries," *J. Electrochem. Soc.*, **138**, 1891 (1991).
3. M. Lerner, S.J. Visco, M. Ue, M.M. Doeff, and L.C. De Jonghe, "Preparation and Discharge Characteristics of Solid Redox Polymerization Electrodes Employing Disulfide Polymers and Copolymers," *Mat. Res. Soc. Symp. Proc.*, **210**, 81 (1991).
4. S.J. Visco, M.M. Doeff, and L.C. De Jonghe, "Current Status of Solid-State Lithium Batteries Employing Solid Redox Polymerization Cathodes," *Symp. Proc. Fifth International Seminar on Lithium Battery Technology and Applications*, Deerfield Beach, Florida, (1991); LBL-30696.
5. S.J. Visco, M.M. Doeff, and L.C. De Jonghe, "Thin-Film Technology for Solid-State Lithium Batteries Employing Solid Redox Polymerization Cathodes," *Symp. Proc. 34th Annual Technical Conference of the Society of Vacuum Coaters*, Philadelphia, PA, 89 (1991).
6. M.M. Doeff, S.J. Visco, and L.C. De Jonghe, "The Use of Redox Polymerization in Lithium Batteries with Liquid Electrolytes," LBL-30466 (1991).

### III. APPLIED SCIENCE RESEARCH

The objectives of this program element are to provide and establish scientific and engineering principles applicable to batteries and electrochemical systems; and to identify, characterize and improve materials and components for use in batteries and electrochemical systems. Projects in this element provide research that supports a wide range of battery systems — alkaline, flow, molten salt, nonaqueous, and solid-electrolyte. Other projects are directed at research on improving the understanding of electrochemical engineering principles, corrosion of battery components, surface analysis of electrodes, and electrocatalysis.

#### A. ELECTRODE CHARACTERIZATION

Zinc is often used as the negative electrode in alkaline cells, and it is this electrode that typically limits the lifetime of these cells. Efforts are underway to identify cell components that will improve the cycle-life performance of the Zn electrode.

#### Surface Morphology of Metals in Electrodeposition

*C.W. Tobias (Lawrence Berkeley Laboratory)*

The objective of this project is to develop a pragmatic understanding of the component processes and their interactions in the macrocrystallization of metals, necessary for the design and optimization of rechargeable galvanic cells. Other objectives are to elucidate the role of electrolyte convection as it affects overpotential behavior and ohmic resistance during gas evolution, and to clarify the effect of concurrent gas evolution on surface morphology in metal deposition processes.

Morphological patterns in thick deposits obtained in flow cells and at rotating disk electrodes (RDEs) are characterized by a Taylor-Hobson profilometer, and by scanning electron microscopy (SEM) and transmission electron microscopy (TEM). Profilometry and photomicrography have been used to evaluate the dependence of leveling performance on orientation of microprofiles in electrodes, in the presence of hydrodynamic flow. In agreement with the model predictions, transverse grooves level more rapidly than those parallel to flow. Coumarin in Ni deposition acts both by blocking metal deposition and by lowering

current efficiency. Leveling by corrosive agents consumed at the transport-limited rate was evaluated using the boundary element method. Significant leveling is demonstrated when the current distribution is dominated by charge-transfer kinetics, and the corrosion rate is comparable to the rate of electrodeposition. Leveling by periodic current reversal is shown to occur when the anodic and cathodic charges passed are identical, and the current distribution is dominated by ohmic resistance during the anodic pulse, and by charge-transfer kinetics during the cathodic pulse.

Deposition of Zn from acid media onto artificially patterned substrates containing micron-scale hemispherical nodules lead to rapid formation of thin, densely spaced striae. The emergence of striations is ascribed to the combination of instantaneous three-dimensional nucleation and fast, concentration-dependent kinetics. The Zn discharge rate is sensitive to small changes in mass transport and ohmic drop in the vicinity of growing nodules. These results, which are summarized in Figure 2, represent the culmination of a multi-year effort to evaluate quantitative effects of various strategies used to impart desirable metal morphologies in rechargeable Zn/halogen batteries.

The mechanism of mossy Zn formation in alkaline media was investigated at a RDE and at a planar electrode in a channel-type flow cell, in the ranges of  $0 < Re < 4000$ ,  $0 < i < 0.05 \text{ A/cm}^2$ , 0.25 and 0.5 M  $\text{Zn}^{2+}$ , and in 3, 6, and 12 M KOH electrolyte. After initially depositing in compact form, moss begins to form around 10- $\mu\text{m}$  nodules, and eventually covers the entire surface. A change in deposition conditions does not reverse the morphology to compact type. Decreasing the zincate ion and increasing the  $\text{OH}^-$  ion concentrations promote the growth of moss. At constant fraction of limiting current, the moss appears more readily when the current density and/or the flow rate is low. Videomicroscopic records have been obtained that show the real-time history of Zn deposits from flowing alkaline zincate media. This information can be used to optimize cell design and operating conditions for electrically rechargeable Zn/air batteries involving flowing electrolytes.

Newly designed micromosaic electrodes (*i.e.*,  $10 \times 10$  quadratic planar matrices of square Pt surface elements with 100- $\mu\text{m}$  edge length, electrically isolated from each other) that are fabricated in-house

## Morphology of Zinc Electrodeposits

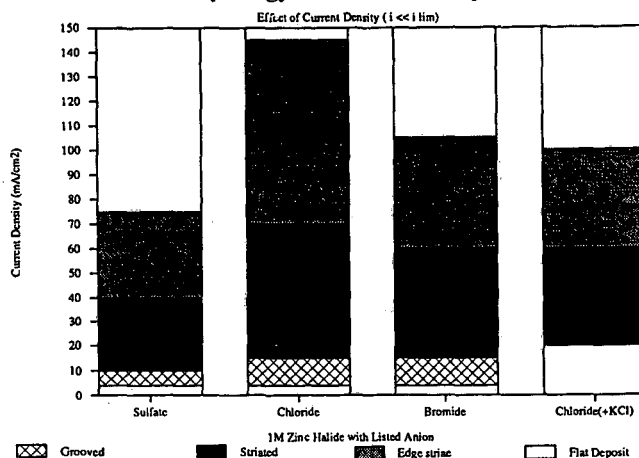


**Figure 2.** Macromorphology of Zn after deposition of  $180 \text{ C/cm}^2$ , as a function of current density and electrolyte composition. The range of current densities over which striae appear varies only slightly, depending on the presence of supporting electrolyte and on the degree of Zn complexation. (XBL 902-448)

used to investigate the effects on the mass transfer boundary layer by a bubble curtain, that rises parallel to a vertical electrode. Measurements of mass-transport enhancement to the diffusion boundary layer demonstrated the presence of two co-temporal enhancement mechanisms: *i*) surface-renewal increases the limiting current within five bubble diameters of the rising column, and *ii*) bubble-induced laminar flows cause a weaker enhancement over a much broader swath. The enhancement by bubble curtains can be predicted with good accuracy by linear superposition of enhancements caused by a single bubble stream (Fig. 3).

The high-speed laser-illuminated photodetector array and associated data acquisition system have been tested by resolving the fast phenomena associated with the coalescence, and separation from the surface, of two electrolytically generated hydrogen bubbles, each of the order of 0.1-cm diameter. In agreement with theoretical predictions, the coalescence event is completed in less than  $10^{-3}$  sec. The electrolysis apparatus built for this purpose contains two opposing microelectrodes on which identical or dissimilar gases may be generated at slow, controlled rates.

## Five Bubble Columns

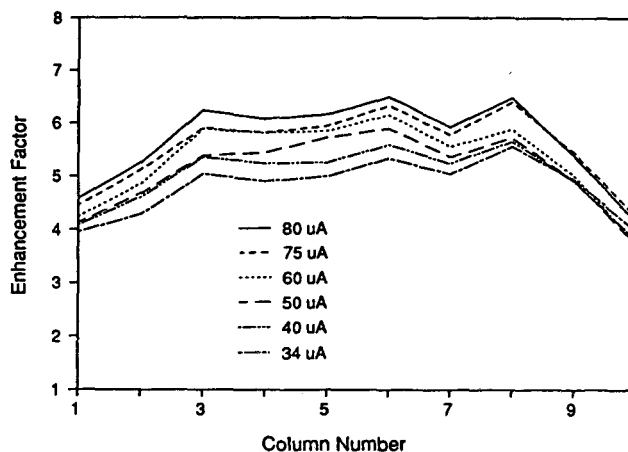


**Figure 3.** Enhancement of transport rates on vertically oriented micro-electrodes by curtain of five parallel hydrogen bubble streams. Distance between streams:  $20 \mu\text{m}$ . Current densities at which bubbles were generated on satellite electrodes were 34 to  $80 \text{ mA/cm}^2$ . Peak enhancement is a factor of six higher than the natural convection limiting current. (XBL 915-1123)

## PUBLICATIONS

1. C.W. Tobias and K.G. Jordan, "The Effect of Inhibitor Transport on Leveling in Electrodeposition," *J. Electrochem. Soc.*, **138**, 1251 (1991).
2. C.W. Tobias and K.G. Jordan, "Simulation of the Role of Convection in Electrodeposition into Microscopic Trenches," *J. Electrochem. Soc.*, **138**, 1933 (1991).
3. C.W. Tobias and K.G. Jordan, "Simulation of the Influence of Corrosive Agents in Electrodeposition on Microprofiles," *J. Electrochem. Soc.*, **138**, 3581 (1991).
4. L. McVay, "Studies of the Development of Mossy Zinc Electrodeposits from Flowing Alkaline Electrolytes," *Ph.D. Thesis*, LBL-30843 (1991).
5. D.P. Sutija, "Micro Scale Mass Transfer Variations During Electrodeposition," *Ph.D. Thesis*, LBL-30825 (1991).

## Battery Materials: Structure and Characterization

J. McBreen (Brookhaven National Laboratory)

The objectives of this project are to elucidate the molecular aspects of materials and electrode processes in batteries and to use this information to develop electrode and electrolyte structures with improved performance and extended life. Work during the year included *in situ* studies of the deposition of mossy Zn from alkaline electrolyte and EXAFS studies of lithium manganese oxides.

*X-ray Absorption Spectroscopy (XAS) Studies of Mossy Zinc Deposits.* Zinc deposition from alkaline zincate electrolytes is unusual in that finely divided mossy deposits are formed at low current densities, whereas in the case of other metals, finely divided deposits are only formed at very high current densities. An *in situ* XAS study of Zn deposition in alkaline electrolyte was started during the year. The studies of Zn deposition were carried out in the thin-layer spectroelectrochemical cell shown in Figure 4. XAS spectra were recorded for the zincate electrolyte, prior to Zn deposition. Zinc was deposited under potentiostatic conditions (-45 or -65 mV vs Zn wire reference electrode) in the thin cavity (~0.5 mm). After sufficient Zn is deposited to fill the cavity above the level of the x-ray window, transmission XAS measurements were made, with the electrode still under potential control. XANES measurements were also recorded on the Zn deposited at -65 mV for one hour after switching the electrode to open circuit. An XAS

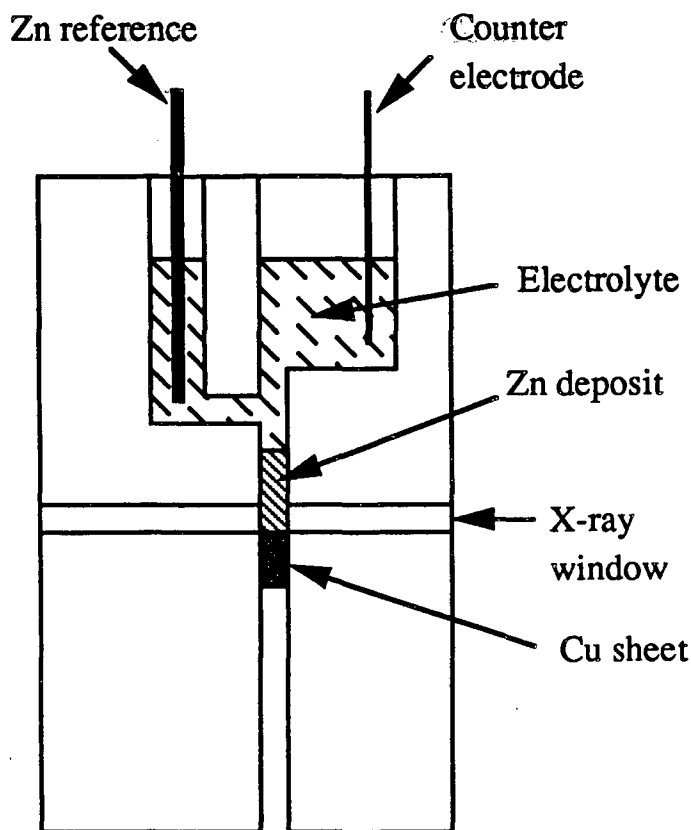


Figure 4. Spectroelectrochemical cell for *in situ* XAS studies of Zn moss deposition.

spectrum was also obtained for Zn foil. The EXAFS results at -65 mV indicate that at this potential the electrolyte in the electrode pores is exhausted of zincate ions and contains only pure KOH electrolyte. However, at -45 mV, there is a Zn-O contribution in the EXAFS, indicating the presence of zincate ions in the electrode pores. The EXAFS results indicate that the deposit at -65 mV is oriented with the c-axis parallel to the lines of current whereas the deposit at -45 mV has a random orientation like that in the Zn foil. A comparison was made of the XANES spectra, for the deposit at -65 mV, taken at various intervals after switching to open circuit. The results are consistent with an increase of zincate ions within the pores of the deposit. As long as there is a deposition at -65 mV, the concentration of zincate ions within the deposit is essentially zero. However, on going to open circuit the zincate concentration within the deposit builds up. This buildup can occur either by diffusion of zincate ions into the electrode pores from the electrolyte on top of the deposit, or by the generation of zincate ions within the pores by concentration-cell effects. The latter are possible, because, on switching to open circuit, the electrolyte in the pores is essentially pure KOH, whereas the electrolyte at the mouth

of the pores, on top of the deposit, is a concentrated zincate solution. The resultant concentration cell would dissolve Zn in the interior of the pores and deposit Zn at the mouth of the pores. The speed with which the concentration of zincate ions in the pores builds up strongly suggests a concentration-cell effect. The cell design may accentuate the effect. However, it will occur in any Zn electrode on termination of charge, and must be taken into account in battery modeling.

**EXAFS Studies of Lithium Manganese Oxides.** A series of  $\text{Li}_x\text{MnO}_2$  compounds was prepared by sintering  $\text{MnO}_2$  (chemical or electrolytic manganese dioxide, CMD or EMD) with either  $\text{LiOH}$  or  $\text{Li}_2\text{CO}_3$  at various temperatures. These were characterized by thermogravimetric analysis and x-ray diffraction. XAS spectra were obtained for several of these compounds including  $\text{LiMn}_2\text{O}_4$ ,  $\text{Li}_2\text{MnO}_3$ , and  $\text{Li}_{0.05}\text{Mn}_2\text{O}_4$ . Spectra were also obtained for  $\text{Mn}$ ,  $\text{MnO}$ ,  $\text{Mn}_2\text{O}_3$ ,  $\text{Mn}_3\text{O}_4$ ,  $\text{KMnO}_4$ , and several types of  $\text{MnO}_2$ . The XANES and EXAFS results for  $\text{LiMn}_2\text{O}_4$  and  $\text{Li}_2\text{MnO}_3$  indicate that, unlike the samples prepared by CMD and EMD, there are no corner-shared  $\text{MnO}_6$  octahedra. Furthermore, the  $\text{MnO}_6$  octahedra are less distorted. The addition of 10% Li to  $\text{MnO}_2$  has minimal effect on either the oxidation state or the structure. The XANES results are consistent with the presence of Mn(IV) in  $\text{Li}_2\text{MnO}_3$  and an average oxidation state of  $\text{Mn}^{+3.5}$  for  $\text{LiMn}_2\text{O}_4$ .

## PUBLICATION

1. D. Guay, G. Tourillon, E. Dartyge, A. Fontaine, J. McBreen, K.I. Pandya, and W.E. O'Grady, "In Situ Time-Resolved EXAFS Study of the Structural Modifications Occurring in Nickel Oxide Electrodes Between Their Fully Oxidized and Reduced State," *J. Electroanal. Chem.*, 305, 83 (1991).

## B. COMPONENTS FOR HIGH-TEMPERATURE CELLS

Superior alternatives to the high-temperature sulfur-polysulfide electrode for Na/S cells are under investigation.

### High-Temperature Cell Research

*E.J. Cairns and F.R. McLarnon (Lawrence Berkeley Laboratory)*

The objectives of this research are to investigate new electrodes, electrolytes and other cell compo-

nents, and to determine the fundamental mechanisms of capacity loss of the electrodes, as well as means for eliminating the losses. Experimental studies of candidate materials for high-temperature cells are augmented by mathematical modeling of electrode behavior during cycling.

The addition of phosphorus to the sulfur electrode of the Na/S cell has been studied *via* equilibrium open-circuit potential measurements. The data allow the structure of the little-studied phase diagram of the Na-P-S system to be inferred, as well as the evaluation of phosphorus as a beneficial additive to the sulfur electrode for energy storage applications. It is anticipated that  $\text{Na/P}_x\text{S}_y$  cells will exhibit higher specific energy than the Na/S cell, owing to the low equivalent weight of phosphorus.

Mixtures with P/S molar ratios ranging from 0.143 to 0.60 and Na mole fractions ranging from 0.0 to 0.4 have been studied at 350 and 400°C. Significantly higher cell voltages (compared to Na/S cells) have been observed, which is a strong indication that phosphorus may be a beneficial additive to the sulfur electrode of energy-storage cells. Also, plots of electromotive force (EMF) vs  $\text{Na}^+$ -ion mole fraction (Fig. 5) indicate that multiple crossings of phase boundaries occur during cell discharge.

To allow re-use of the costly  $\text{Na}^+$ -ion-conducting ceramic ( $\beta''\text{-Al}_2\text{O}_3$ ) electrolyte, a cell was designed

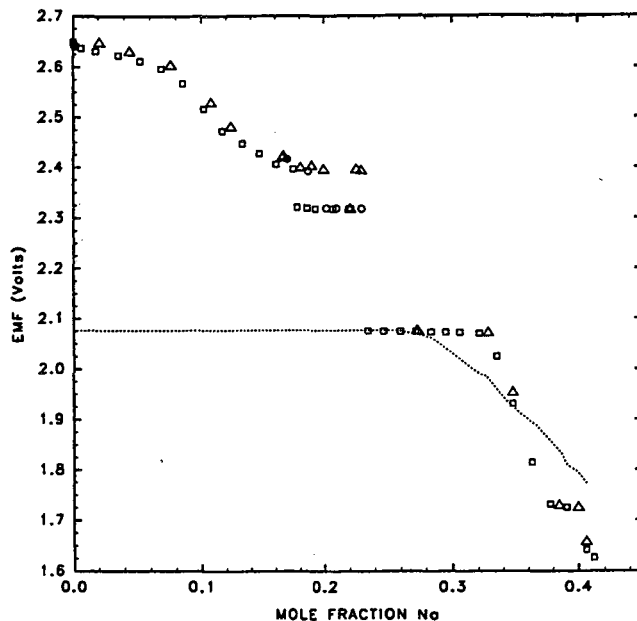


Figure 5. Plot of cell potential (EMF) vs Na mole fraction in P-S melt within sodium/phosphorous-sulfur cell.  $\square$  1st discharge,  $\Delta$  charge,  $\circ$  discharge, ——— Na/S at 350°C

which could be disassembled after use with the electrolyte intact. The parts of the cell exposed to the corrosive phosphorus and sulfur environment were constructed of Mo, but otherwise Inconel 718 and A286 steels were used to impart strength at high temperature. Seals were maintained from 28 to 500°C using "C-ring" gaskets and disk springs. Graphite-coated Al gaskets provided hermetic and demountable seals.

## C. CORROSION PROCESSES IN HIGH-SPECIFIC-ENERGY CELLS

These projects aim to develop low-cost containers and current-collector materials for use in nonaqueous, alkali-sulfur, and other molten-salt cells.

### Corrosion-Resistant Coatings for High-Temperature High-Sulfur-Activity Applications

*J.R. Selman (Illinois Institute of Technology)*

The objective of this research is to develop corrosion-resistant coatings for cell components that are exposed to high-sulfur-activity environments in Na/S and Li/FeS<sub>2</sub> batteries. The efforts are directed at producing dense and pore-free Mo<sub>2</sub>C coatings on low-carbon steel, and to determine the correlation of coating quality with process parameters such as temperature, current density, melt composition, etc.

*Optimized Deposition of Molybdenum and Molybdenum Carbide.* Coatings of Mo and Mo<sub>2</sub>C were prepared by molten salt electrochemical deposition (MSECD). Several different bath compositions were utilized with ~8-10 mol% alkali molybdate and variable amount of alkali carbonate. Commercially available laboratory chemicals were first dried at 200-300°C for 2-3 h to remove as much moisture as possible. Then the chemicals were weighed and mixed to give the desired electrolyte composition. As a second step in the purification process, the melt was electrolyzed (1.5-2.0 V at 650°C) between two carbon electrodes until the current dropped to a low constant value, which signified that the remaining moisture was completely removed. Experiments performed without pre-electrolysis of the electrolyte usually gave non-reproducible results. After pre-electrolysis of the melt, coatings of a more reproducible quality were obtained. Coatings of an even better quality were obtained with a bath containing non-Li alkali molybdates and carbonates. Adding 3-8 mol% Na<sub>2</sub>B<sub>4</sub>O<sub>7</sub> to the basic non-Li bath composition was observed to yield significant improvements in the morphology

and quality of the coatings. These bath compositions produce a more uniform, small-grain-size coating, and they do not require extensive purification because they are apparently not very sensitive to moisture.

The working temperature was varied from 900 to 1000°C; below 850°C no deposit was observed. Non-Li electrolytes, in all cases, required higher working temperatures. Baths that contain borate salt require even higher temperatures, by 50-80°C. Such an increase of temperature causes significant changes; larger grain sizes are found at higher temperatures.

Both constant-current and reverse- and/or pulse-current patterns were applied during plating. The latter produce coatings with smaller grain size than the former, at the same working temperature. Reverse/pulse-current plating also makes higher current densities possible and appears to be more effective in generating good-quality coatings. Generally, the cross section of the samples indicate a virtually dense pore-free coating of approximately uniform thickness, even with an irregular substrate profile. The deposit consisted of two zones: *i*) a region near the substrate interface containing both Fe and Mo, probably a Mo interlayer and/or Fe-Mo alloy formed by diffusion; and *ii*) a zone further out, which constitutes the true carbide coating.

*Preparation of Mo and Mo<sub>2</sub>C by Plasma-Enhanced Chemical Vapor Deposition.* Plasma-enhanced chemical vapor deposition (PECVD) is a new technique for preparing thin protective films at much lower temperatures than those used by thermally driven CVD. Lower temperatures are needed in PECVD because the addition of plasma energy in the form of a glow discharge creates highly reactive species in the CVD environment. An effort was undertaken to deposit Mo and Mo<sub>2</sub>C films on a small substrate (2.54 × 3.81 cm). The following experimental parameters were varied: pressure (P), temperature (T), RF power, time (t), and gas flow rate (F). Using an orthogonal factorial design, a series of experiments was carried out to investigate the effect of the evaporation rate of Mo(CO)<sub>6</sub> as a precursor. The substrate and Mo(CO)<sub>6</sub> powder were accurately weighed (precision 10<sup>-4</sup> g) before and after the discharge process to estimate the approximate deposition rate of Mo or Mo<sub>2</sub>C and the evaporation rate of Mo(CO)<sub>6</sub>.

From the weight gain of the substrate, initial conclusions were drawn about the optimal conditions for achieving the maximum evaporation rate, deposition rate, and thickness. The analysis clearly shows that the factor which affects the deposition rate most is the flow rate of the Ar carrier gas. The deposition rate may be increased strongly if the introduction of Ar

into the reaction chamber can be avoided; the carrier gas dilutes the concentration of  $\text{Mo}(\text{CO})_6$  above the substrate and decreases the deposition rate of Mo or  $\text{Mo}_2\text{C}$ . These results indicate that it is possible to directly evaporate  $\text{Mo}(\text{CO})_6$ , i.e.,  $\text{Mo}(\text{CO})_6$  is used as a discharge medium.

The second factor is the pressure in the reaction chamber. The lower the pressure, the higher the deposition rate, because the lower pressure promotes evaporation of  $\text{Mo}(\text{CO})_6$  and its concentration in the chamber increases. Other important factors are the temperature and power density in the chamber. If the temperature and power density increase, the concentrations of radicals and gaseous ions also increase. This should accelerate deposition by increasing the evaporation rate. The deposition time is not an important factor; deposit thickness would be expected to increase with time.

Analysis of the composition and microscopic morphology examination of the film were carried out. In general, the films were smooth and the thickness was slightly larger than calculated from the weight gain, assuming pure Mo. Their morphology and the film properties are now being evaluated. It is inferred that the film thickness is in the range of about 10  $\mu\text{m}$ .

## Improved Container Electrode Coating for Na/S Battery Systems

*T. Hunt (Environmental Research Institute of Michigan)*

The objective of this project is to develop improved corrosion-resistant coatings for high-temperature secondary batteries by sputter-deposition techniques. At the outset of this effort the literature on coatings for corrosion protection of the container electrode surface in Na/S cells, and in particular, the results obtained at Ford Motor Company were re-examined. The tests conducted at Ford indicated that sputtered TiN-coated Al was unaffected by the high-sulfur activity (samples immersed in a polysulfide bath for 72 days) and the imposed voltage excursions, which approximated the voltage range in Na/S cells. These preliminary results were sufficiently encouraging that further development of TiN-coated materials was undertaken in this project.

To accelerate the preparation of the initial samples, it was decided to use the reactive-sputtering apparatus at Ford, in which the original TiN-coated Al samples were prepared. Sputtering runs verified that TiN could be deposited with the same quality that was evident in the previous, successful corrosion experiments on Al substrates. Test samples that were

prepared on glass slides were used to calibrate thickness vs deposition time and power, and to look for stresses in the deposited films. Methods for pre-sputtering, glow-discharge cleaning, and voltage biasing of substrates to enhance adhesion were explored in consultation with David Hoffman (Ford) and Norman Draeger (Midwest Research Technologies).

The possibility of utilizing non-reactive sputtering, which may possibly require less-critical operating conditions, were examined in several trial deposition runs using a commercial TiN sputtering target. The first trials using direct current (D.C.) magnetron sputtering with a 3-inch diameter sintered TiN target (purchased from Angstrom Sciences) were unsuccessful. Modifications were then made to the radio frequency (R.F.) sputtering system to accommodate smaller targets, and sputtering tests were conducted in the R.F. mode. Variable results were obtained in these tests; the appropriate color was achieved, but the stresses in the deposited films were excessive even at modest film thicknesses. High compressive film stresses were inferred from the curvature imposed upon thin glass cover slips on which the films were deposited simultaneously. The films that were deposited on Al appear to have much better adhesion than the films on glass. A profilometer was used to measure the thickness of films deposited simultaneously as "control pieces." Reactive sputtering is anticipated for the preparation of the majority of coatings that will be examined. However, experiments also will be conducted to understand the stress regimes on coatings obtained by R.F. sputtering, because control of the deposition parameters for reactive sputtering appears to be more demanding.

Because the sputtering system at Ford was scheduled to be dismantled and cleaned in early 1992, assembly of a reactive-sputtering system was initiated at ERIM. The essential components (flow meters and controller for the reactive gases) were purchased, and the design of a bell-jar adapter to connect a 30-inch stainless steel bell jar to a 6-inch diffusion pumped station was started.

## Corrosion, Passivity, and Breakdown of Alloys Used in High-Energy Batteries

*J. Kruger (The Johns Hopkins University)*

The objective of this project is to investigate the phenomena of passivation and its breakdown on metals and alloys in nonaqueous solvents for rechargeable Li batteries. The formation and stability of passive films is important for the sustained integrity of

containment materials used in high-energy batteries. This study is specifically concerned with the nature, formation mechanisms, and the mechanism of breakdown of passive films that exist on alloys in nonaqueous solvents. The effort in 1991 has concentrated on the behavior of 1018 carbon steel and high-purity iron in dimethoxyethane (DME) and  $\text{LiAsF}_6$  supporting electrolyte.

Pure iron and 1018 carbon steel display extensive and stable passive regions in anhydrous 0.5 M  $\text{LiAsF}_6/\text{DME}$ . Iron in a nominally dry  $\text{LiAsF}_6/\text{DME}$  solution containing less than 100-ppm water has a breakdown potential of 1300 mV (*vs* saturated calomel electrode, SCE), whereas 1018 carbon steel displays a breakdown potential of 1050 mV (*vs* SCE) in the same solution. The incremental addition of 50-, 100-, and 200-ppm water raised the breakdown potential of both alloys to 1750 mV. In this passive region, several distinct passivation mechanisms are operative. Solvent chemisorption provides passivity up to 850 mV. Between 850 and 1100 mV on carbon steel, and between 850 and 1250 mV on Fe, another passivation mechanism appears to be operative, other than the formation of an inorganic salt film such as that observed in propylene carbonate (PC) solutions. Our experiments indicate that the most plausible explanation of the observed behavior in this potential range is that DME is chemically or electrochemically transformed, in the presence of  $\text{AsF}_6^-$  or a derivative, to a chemical intermediate that adsorbs on the carbon steel and provides a passive film.

At potentials in the vicinity of 1300 mV for Fe and 1100 mV for carbon steel, where an enormous quantity of charge is passed during repassivation, there is evidence that suggests a carbon-based polymer film is formed. Although the amount of charge passed would seem to be consistent with dissolution followed by precipitation of a salt film, this possibility can be ruled out based on the following arguments. First, x-ray microanalysis and x-ray photoelectron spectroscopy (XPS) analysis fail to show any evidence of As in the scratch. Arsenic would most certainly be a component in a salt film because  $\text{AsF}_6^-$  is the only anion in solution. Incidentally, the lack of As in the scratch most likely excludes the possible formation of an inorganic polymer film. Second, there is no visible dissolution, no discoloration of the solution, and no evidence of severe electrochemical attack that would be expected if the Fe surface was undergoing appreciable oxidation. A bare metal surface is apparently necessary for the electropolymerization reaction to initiate. It is likely that the adsorbed precursor film

formed at 850-1250 mV effectively inhibits charge transfer to a degree that polymerization cannot proceed. The fact that the same amount of charge is passed on stepping to either 1200 or 1300 mV lends further evidence that polymerization requires a clean metal surface. If the initiation of the polymerization reaction is dependent only on potential, initiation would be expected to proceed from the moment the potential was stepped from open circuit to 1300 mV. This does not happen.

Trace amounts of water and  $\text{LiAsF}_6$  act as co-catalysts for polymerization. The results indicate that the polymerization reaction is enhanced by a small increase in water content. The polymerization does not proceed and the passive region is diminished when salts other than  $\text{LiAsF}_6$  are used. Electropolymerization in  $\text{LiAsF}_6/\text{DME}$  is similar to the polymerization found in 1,3-dioxolane with  $\text{LiAsF}_6$ .

For binary DME/ $\text{H}_2\text{O}$  mixtures (0-50 mol% DME), no unstable passivity materializes in the passive regions of iron or carbon. The passive currents remain steady or decrease for experiments of up to one hour at constant potential. Mixed solutions above 50 mol% DME display no active/passive transition although the nose of the curve may be masked by the cathodic reaction.

Because sulfides, a Lewis base, appear to restrict the polymerization process on carbon steel, the presence of another potential Lewis base such as the chloride ion was added to observe its effects in 0.5 M  $\text{LiAsF}_6/\text{DME}$ . A saturated solution of  $\text{LiCl}/\text{DME}$  was added to 0.5 M  $\text{LiAsF}_6$  solutions of DME/ $\text{H}_2\text{O}$  ranging from nominally dry to 50 mol% DME. The presence of up to 0.012 M  $\text{LiCl}$  in dry 0.5 M  $\text{LiAsF}_6/\text{DME}$  solutions did not reverse the polymerization process nor lower the breakdown potential. This may be caused by the inability of  $\text{LiCl}$  to dissociate in dry DME and act as a Lewis base. However, water contents from 2000 ppm to 50 mol%, which would enhance salt dissociation, did not appear to alter the observations in dry  $\text{LiAsF}_6/\text{DME}$ .

## PUBLICATIONS

1. D.A. Shifler, P.J. Moran, J. Kruger, "The Passivity of Iron and Carbon Steel in Anhydrous Propylene Carbonate Solution", *Corrosion Science*, **32**, 475 (1991).
2. D.A. Shifler, P.J. Moran, J. Kruger, "The Passivity of 304 Stainless Steel in Propylene Carbonate Solutions," *J. Electrochem. Soc.*, **139**, 54 (1992).

## D. COMPONENTS FOR AMBIENT-TEMPERATURE NONAQUEOUS CELLS

Metal/electrolyte combinations that improve the rechargeability of ambient-temperature, nonaqueous cells are under investigation.

### Spectroscopic Studies of the Passive Film on Alkali and Alkaline Earth Metals in Nonaqueous Solvents: A Surface Science Approach

D.A. Scherson (Case Western Reserve University)

The main objective of this research is to elucidate the structure of passive films that form on alkali and alkaline earth metals in nonaqueous solvents. The interactions between Li and tetrahydrofuran (THF) have been investigated in ultrahigh vacuum (UHV) using Fourier Transform Infrared Reflectance Absorption Spectroscopy (FTIRRAS), a Quartz Crystal Microbalance (QCM), Auger Electron Spectroscopy (AES), and Temperature Programmed Desorption (TPD).

#### A. FTIRRAS Studies in UHV

The spectroscopic measurements were conducted in a specially designed UHV/FTIRRAS/QCM chamber that is equipped with Li (SAES Getters) and Au sources, and gas-dosing capabilities. The results of careful FTIR/QCM experiments indicate that this system is sensitive enough to detect a single monolayer of THF adsorbed on Au. Figure 6 shows the normalized difference FTIRRAS spectra ( $\Delta R/R$  vs wavenumber) of a Li-THF layer that is formed by the simultaneous codeposition of the two constituents onto a Au-coated substrate at a temperature of  $\sim 90$  K. In this case,  $\Delta R/R = (R_{\text{sample}} - R_{\text{ref}})/R_{\text{ref}}$  where  $R_{\text{sample}}$  and  $R_{\text{ref}}$  are the spectra obtained in the presence and in the absence (bare Au) of the Li-THF overlayer, respectively. Although it was not possible to determine the exact proportion of Li and THF in the mixture, the total amount of material, as measured *in situ* by the QCM, was on the order of five monolayers. All the peaks observed in the spectra, including the prominent peaks at 1061 and 914  $\text{cm}^{-1}$  (associated with the asymmetric and symmetric ring stretches), are characteristic of THF. None of these features could be observed in the FTIRRAS spectra obtained at a temperature high enough (160 K) to induce bulk desorption of THF. Instead, the bare-Au referenced-spectrum revealed the presence of new species on the surface that

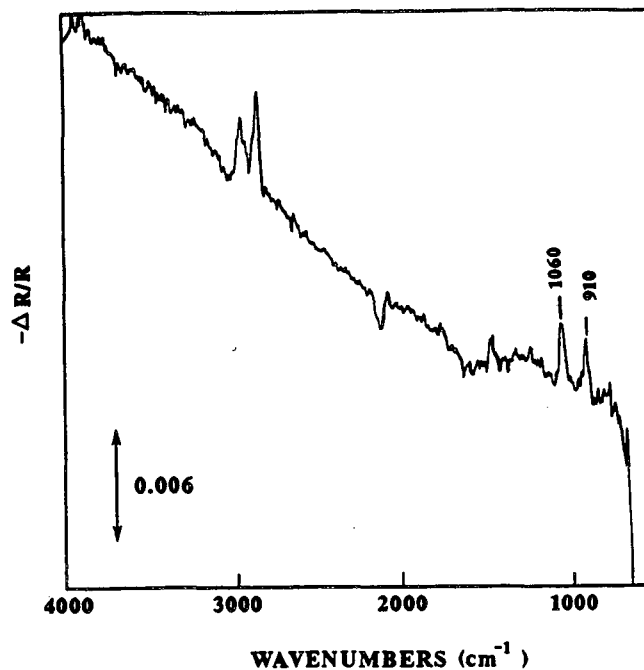


Figure 6. FTIRRAS spectrum of a Li-THF layer formed by simultaneous codeposition of the two constituents on a freshly coated Au surface at 90 K.

most certainly originate from the reaction between Li and THF (Fig. 7). For example, the peak at 1053  $\text{cm}^{-1}$  is consistent with a CO alcohol moiety whereas that at 1110  $\text{cm}^{-1}$  can be ascribed to a stretch of an ether-linkage of the type  $\text{CH}_3\text{O}$  and  $\text{CH}_2\text{O}$ .

Similar results were obtained in experiments in which the Li layer was deposited first on the Au surface, and then followed immediately by several layers of THF. In this experiment, at least one of the reaction products of THF and Li appears to be lithium alkoxide. Also examined were interfaces prepared by depositing (in sequence) first THF and then Li on a bare Au surface. Peaks at 872, 1490, 1400 and 1651  $\text{cm}^{-1}$  that are characteristic of organic lithium carbonates were observed after raising the temperature to 160 K. This provides clear evidence for a reaction between adventitious carbon dioxide in the chamber and lithium alkoxide produced by the interaction between Li and THF.

#### B. AES and TPD Measurements

The AES spectrum of a freshly deposited Li layer on a clean Ag substrate (Fig. 8) displayed characteristic features of clean Li, including the peak at 51 eV (KLL transition) and that at 80 eV which is attributed to a doubly ionized K-shell transition. This surface

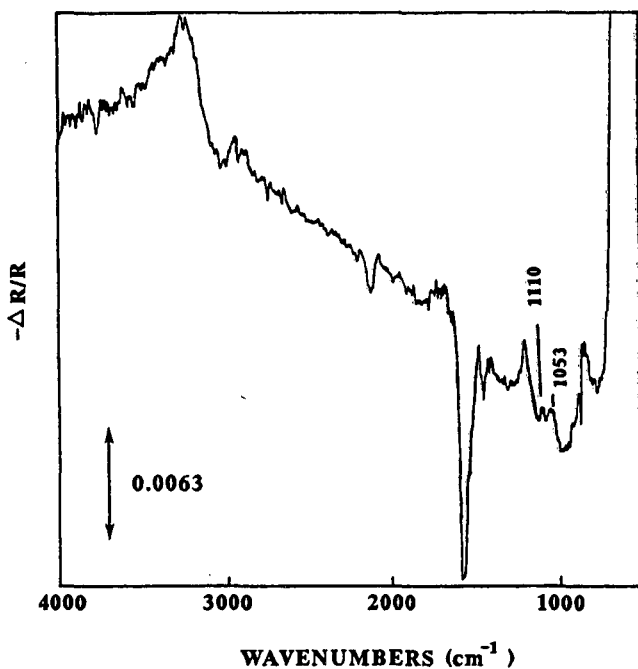


Figure 7. FTIRAS spectrum of the surface in Fig. 6 after raising the temperature to 160 K.

was very sensitive to the presence of impurities. In particular, the peak at 51 eV was found to broaden and then to shift to about 42 eV after leaving a freshly deposited Li surface in the chamber for several hours.

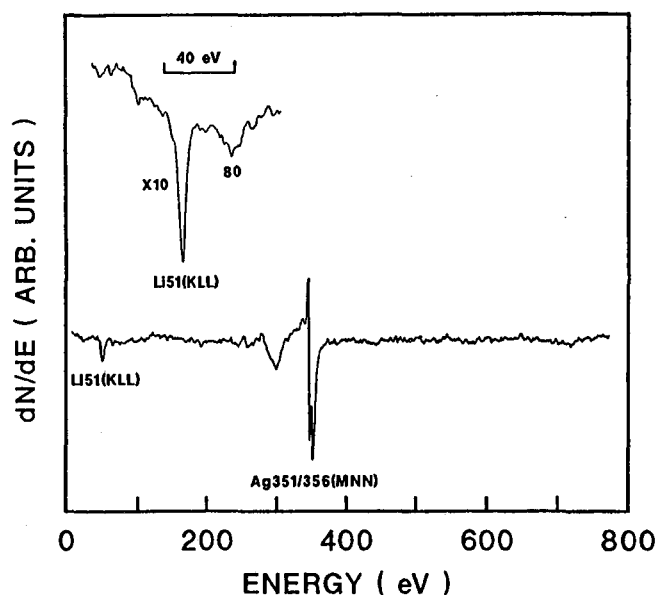


Figure 8. AES spectrum of a Li-covered Ag surface (50% Li). The inset displays another spectrum in the region of the Li(KLL) transition recorded at much higher sensitivity.

If the UHV exposure was extended for about 12 h, new features at 23.5, 36, 50, 69 and 80 eV emerged which are ascribed to a mixture of Li-O and Li-CO<sub>3</sub> species.

No TPD peaks could be detected at higher temperatures after exposing a clean Ag(poly) at ~300 K to several Langmuirs of THF. Experiments in which the THF was adsorbed at 98 K, however, yielded sharp TPD peaks associated with the normal desorption of THF ( $m/e = 48, 80, 44, 32$ ) at a temperature of 165 K, followed by a poorly defined shoulder. The desorption kinetics for this feature were found to be zero-order in THF and the relative ratios of these peaks are in agreement with those expected for "normal" THF. This is consistent with the (bulk) desorption of THF and in accordance with the FTIR/UHV data. Very small features could also be observed at higher temperatures (370, 506, 683 and 880 K), the nature of which have not been identified yet.

The adsorption of THF on Li/Ag(poly) was found to be negligible at ~300 K, yielding only very minor and ill-defined peaks of THF fragments at higher temperatures in the TPD spectra. The TPD spectra of 10-L THF condensed on a Li (~3 monolayers)/Ag surface at 98 K showed features at 165 (bulk THF), 225, 340, 442 and 750 K (Fig. 9). Experiments in which the amount of Li was varied indicated that the temperature of the peak at 225 K (first-order kinetics in THF) was not a function of the Li coverage, although its

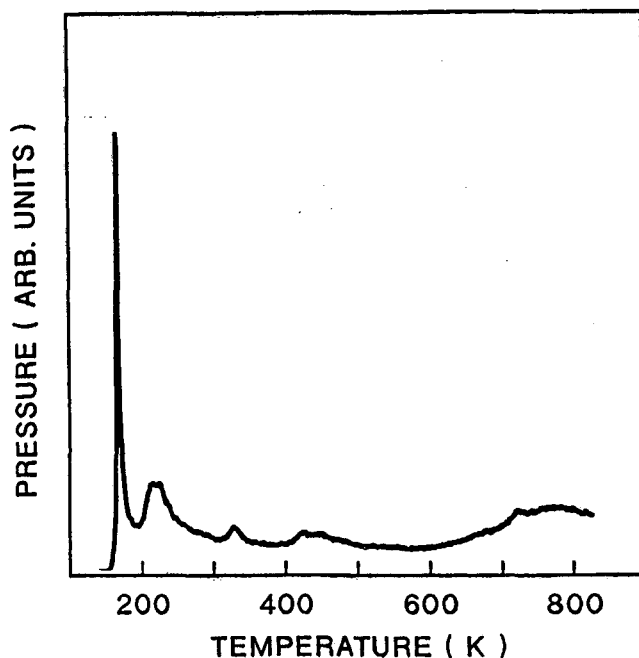


Figure 9. TPD spectrum of a Li-covered Ag surface exposed to 10 L D-THF at 98 K.

amplitude increased as the amount of Li increased. This strongly suggests that this peak is indeed associated with a Li-THF interaction. The peaks at 340, 442 and 750 K shifted to lower temperatures when the Li coverage was increased. This implies that these features are affected both by Li and Ag and/or that the order of their desorption kinetics is different from those of the peaks at 175 and 225 K. With the exception of the 165 K peak, all other features showed relative m/e ratios which deviated significantly from those of "normal" THF.

Measurements were also conducted in which Li and THF were coadsorbed simultaneously on the Ag surface to enhance possible Li-THF interactions. This surface displayed TPD features similar to those obtained by sequential deposition (Fig. 10), except that the amplitudes of the features (other than the peak at 175 K) were much larger than those observed in the run involving sequential adsorption. Much larger peaks at 43, 442 and 750 K could also be observed when the time elapsed between the codeposition and TPD was extended to about 45 minutes. Perhaps the strongest evidence in favor of a Li-THF reaction is provided by the presence of oxygen on the Ag surface after the surface had been heated to about 950 to 1000°C.

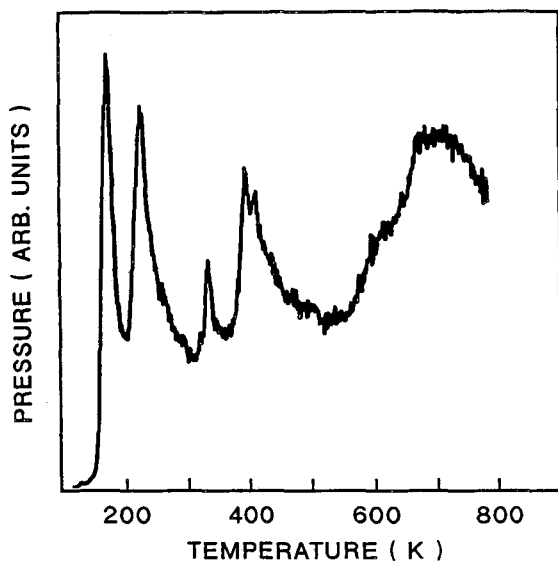


Figure 10. TPD spectrum of a Ag surface after exposure to 10 L of THF and Li at 98 K.

## ***In Situ* Spectroscopic Applications to the Study of Rechargeable Lithium Batteries**

*D.A. Scherson (Case Western Reserve University)*

This project, initiated in 1991, uses *in situ* spectroscopic techniques to investigate charge/discharge reactions of Li at Li/SPE interfaces. Techniques have been developed and implemented to investigate the Li electrode in PEO electrolytes under conditions of direct relevance to rechargeable Li/polymer battery technology.

Most of the operations involved in the preparation of PEO films were performed in a dry glove box (Vacuum Atmospheres with Dri-train HE-493) under an Ar atmosphere. All glassware and other utensils were scrupulously cleaned and then dried at 100°C just before being introduced into the dry box. Acetonitrile (Aldrich) was distilled and stored in molecular sieves (8-12 mesh). LiClO<sub>4</sub>(Aldrich) and LiAsF<sub>6</sub>(Aldrich) were recrystallized and subsequently dried under vacuum. After purification, all chemicals were stored in the dry box.

Mixtures containing 12 g PEO (Aldrich, MW = 600,000, dried and used without further purification) and 0.8 g LiClO<sub>4</sub> (or 1.5 g LiAsF<sub>6</sub>) were placed in a beaker. The relative amounts of polymer to salt are just sufficient to yield a Li<sup>+</sup>/PEO ratio of 36. Acetonitrile was then added to the beaker to reach a total volume of 120 mL and the mixture stirred with a Teflon-covered rod until it became homogeneous. A Teflon-coated magnetic bar was then added to the beaker and the stirring was resumed for 2-3 days until the solution turned smooth and translucent in appearance. The total amount of liquid was always kept at 120 mL by adding more neat acetonitrile if necessary.

Li-salt/PEO films were cast onto thoroughly cleaned and dried glass plates (3" × 3") using a film applicator (Pacific Scientific), selecting a thickness of 30 mils. A Petri dish was then placed on top of the film leaving a gap for gas flow. After about 3-4 hours, most of the solvent evaporates and the films turn opaque. At this stage the films were cut, released from the glass, and placed in Al foil envelopes. The films were allowed to dry for two days in the dry box and later in the intermediate (glove box) antechamber under vacuum for 6 h. Materials prepared in this fashion could be stored indefinitely in the glove box without deterioration. Before use, however, the films (~2-mils thick) were placed onto Teflon slides and dried further at ~95°C and under reduced pressure for two days in an oven external to the glove box. Prior to the transfer, the supported films were placed

in polyethylene bottles to avoid prolonged exposure to the atmosphere. After the vacuum oven was back-filled with ultra-high purity (UHP) Ar, the bottles were tightly capped and transferred back to the glove box.

Cyclic voltammetry measurements were conducted in a specially designed electrochemical cell using vapor-deposited Au films (~100-nm thickness) on glass slides as working electrodes. The voltammetric cycles were always initiated at or near the open circuit potential (OCP) at a scan rate of 5 mV/sec. In most cases, the Li foil was used as a single reference/counter electrode. Except for a shift in potential, the results obtained employing a two-electrode approach were essentially identical to those obtained using a reference electrode prepared *in situ* by electrodepositing Li on the isolated Au region.

Figure 11 shows a series of voltammetric scans obtained in sequence for a vapor-deposited Au electrode in LiClO<sub>4</sub>/PEO at 55°C using a two-electrode cell configuration. Prior to recording these curves, the

electrode was cycled according to the program given schematically in the insert. For the subsequent scans, the negative limit was extended to 0.5 (Curve A), 0.37 (Curve B) and 0.0 V (Curve C), respectively, maintaining the positive limit at 2.0 V. As can be clearly seen, the voltammetric curves display two features in the scan in the negative and positive directions at a potential more positive than that required for bulk Li deposition. In analogy with the results obtained in organic solvents, these peaks can be attributed to UPD Li on Au. Further supportive evidence is provided by the charge under the current-voltage curve observed in the scan in the positive direction (Curve B) which yielded a value very close to that expected for the discharge of a single electron on a cm<sup>2</sup> of Au surface. The steep increase in the cathodic current observed in Curve C at about 0.25 V can be ascribed to the bulk deposition of Li which yields, upon reversing the scan, well-defined stripping characterized by the peaks centered at 0.5 V.

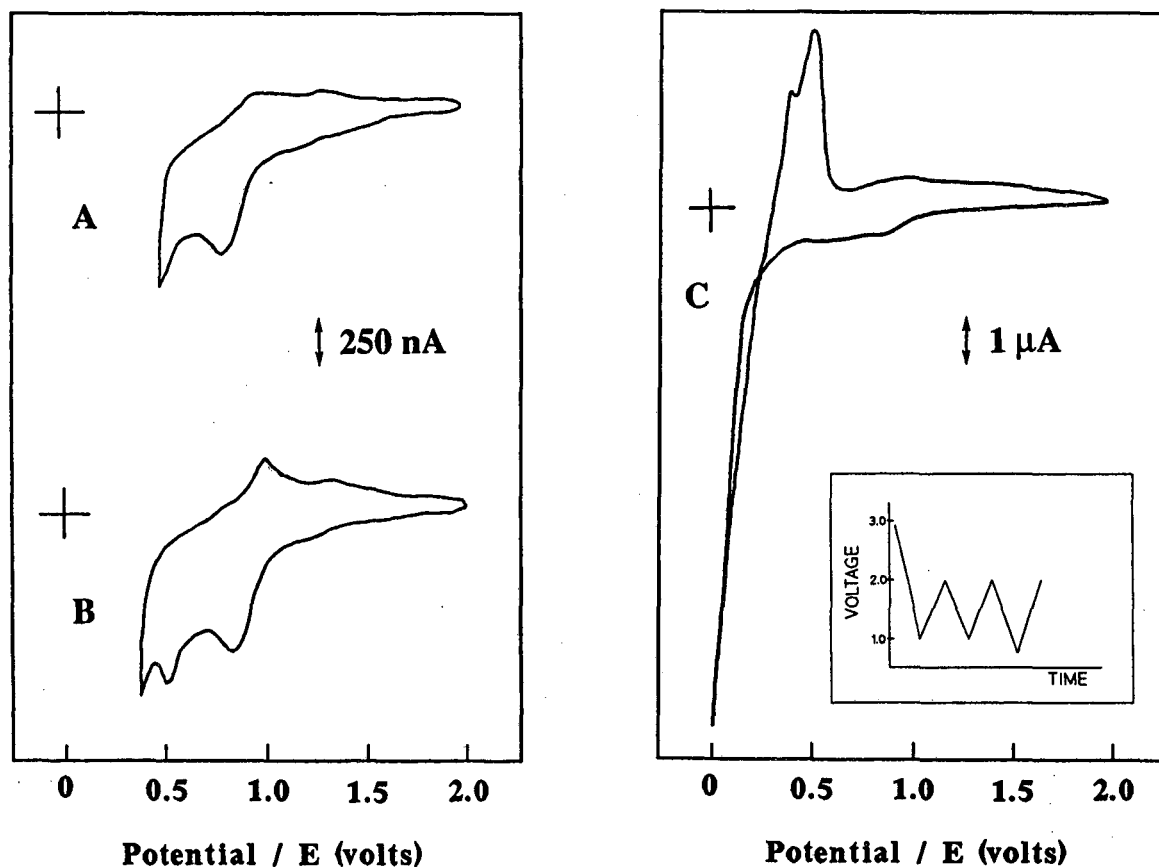


Figure 11. Series of voltammetric cycles obtained in sequence for a vapor-deposited Au electrode in LiClO<sub>4</sub>/PEO at 55°C using a two-electrode cell configuration. Electrode Area: 0.31 cm<sup>2</sup>. Curve A: Third Cycle; Curve B: Fourth Cycle; Curve C: Fifth Cycle. Prior to recording these curves, the electrode was cycled according to the program given schematically in the Insert.

## Polymeric Electrolytes for Ambient-Temperature Batteries

G.C. Farrington (University of Pennsylvania)

This program investigates the chemical and electrochemical characteristics of polymeric electrolytes for use in high-specific-energy batteries. The investigations this year focused on exploring new compositions of polymer electrolytes which have excellent physical and chemical properties, as well as high ionic conductivity. The polymeric electrolytes were formed by radiation polymerization of mixtures of acrylate oligomers containing organic plasticizers and dissolved salt, 1 M LiAsF<sub>6</sub>. Mixtures of ethylene carbonate (EC) and propylene carbonate (PC) were used as the plasticizers in the proportions EC:PC (100:0, 75:25, 50:50, 25:75, 0:100 by wt%).

The mechanical properties of the new electrolytes are excellent. They are rubbery and clear, unlike electrolytes formed simply with either pure EC or PC, which are brittle and milky. A detailed study of the thermal stability of all of the polymer compositions was carried out. It showed that the polymeric electrolyte with the composition 50:50 EC:PC is the most stable thermally and had a weight-loss of only 0.3% at 100°C, whereas the composition containing pure PC is the least stable, with 3.28% weight-loss at the same temperature. The other compositions have stabilities in between these values. In addition, the decomposition of the polymer electrolyte containing mixed EC/PC and pure EC as the plasticizer occurred in two steps where the electrolyte containing pure PC occurred in a one-step process.

The differential scanning calorimetry (DSC) studies showed that polymer electrolytes with pure EC have two melting peaks, around 26 and 30°C and a T<sub>g</sub> of about -65°C. Thus, they are partially crystalline at room temperature. When 25 wt% PC is added to EC (75:25), both melting peaks shift to considerably lower values, 8 and 15°C, respectively. Not only do the melting peaks shift to lower values, but the T<sub>g</sub> also shifts to about -75°C. As a result, the electrolyte is amorphous at room temperature but partially crystalline at sub-ambient temperatures. When 50 wt% PC is added to EC, both the melting peaks disappear completely, rendering the electrolyte completely amorphous and the T<sub>g</sub> shifts to an even lower temperature of about -94°C. A further increase in the EC/PC ratio does not change the DSC results. Hence the electrolyte compositions with ≥ 50 PC contents are completely amorphous from -90 to 150 C.

The room-temperature ionic conductivities of the different polymeric electrolytes containing EC/PC

were also studied. The electrolyte with pure PC has the highest conductivity, about  $2.3 \times 10^{-3}$  S/cm and that with pure EC the lowest, about  $5 \times 10^{-4}$  S/cm. This difference is expected, since the composition with pure EC is partially crystalline at room temperature, which results in a lower conductivity. The conductivities of polymeric electrolytes that contain mixed compositions fall between these two limits. The conductivities of 50:50 and higher PC content are only marginally lower ( $>8.0 \times 10^{-4}$  S/cm) than that formed with pure PC.

Cyclic voltammetric studies on symmetrical Li/SPE/Li cells show that all the electrolyte compositions studied appear reasonably stable to about +4.0 V vs Li/Li<sup>+</sup>. The Li redox process is reversible and reproducible after the first cycle at a scan rate of 1 to 10 mV/s for compositions 50:50, 25:75, and pure PC, but less reversible for electrolytes containing pure EC and 75:25 mixtures. Hence, judged on the criterion of Li cyclability, the mixed compositions of 50:50 and higher PC contents are quite promising for secondary Li battery applications over a range of temperature from -60 to 100°C.

## Solid Polymer Electrolytes for Rechargeable Batteries

S. Narang (SRI International)

The objective of this research is to develop advanced ion-conducting polymers that can be used as SPEs in high-energy, rechargeable solid-state batteries. Batteries of this type (e.g., Li/SPE/MnO<sub>2</sub> or Li/SPE/V<sub>6</sub>O<sub>13</sub>) promise virtually maintenance-free, reliable operation over many hundreds of cycles if certain physicochemical problems can be overcome. Some of the most important problems are summarized as follows: *i*) low mobility of Li<sup>+</sup> ions in the SPE, *ii*) difficulty of maintaining an intimate contact between SPE/Li negative and SPE/intercalation positive electrode, *iii*) occasional growth of a Li dendrite that penetrates the SPE on recharging, *iv*) low utilization of the positive electrode on rapid charging, and *v*) poor long-term stability of the SPE at operating temperature (e.g., 80-100°C).

Poly(ethyleneoxide) or poly(propyleneoxide) (PPO) with Li complexes exhibit ionic conductivities that are suitable for high-energy, rechargeable batteries only above 100°C. In the past few years polymers that have better conductivity than PEO at room temperature, such as polyphosphazene-based ionic conductors, have been developed. However, their ionic

conductivities are still too low, and these electrolytes do not provide flexible, dimensionally stable films, which are needed to meet DOE/USABC power requirements (>100 W/kg sustained power).

Polymer electrolytes with significantly higher Li ion conductivity than PEO were developed by systematically replacing oxygen atoms with sulfur atoms in PEO-type structures. This substitution reduces the strong hard-acid hard-base interaction between Li ion and ether oxygens of PEO, while retaining the favorable helical conformation of the polymer backbone. Dimensionally stable polymer electrolyte films have been prepared by *in situ* polymerization of tetraethylorthosilicate (TEOS) in the presence of the Li complex of sulfur-substituted PEO. The linear polymer electrolyte chains entangle into the crosslinked chains of the silicate polymer, conferring good dimensional stability and high ionic conductivity. The best-performing polymer electrolyte, obtained from sulfur-substituted PEO (16.7% sulfur substitution) and TEOS with a plasticizer, showed a conductivity of  $7.5 \times 10^{-4}$  S/cm in a Li/Li cell.

Single-ion conducting polymer electrolytes based on poly(siloxane) and poly(phosphazene) backbones were synthesized and characterized. The unique feature of this effort is the introduction of perfluoroalkylsulfonate functional groups into the polymer backbone. Phosphazene-based and siloxane-based single-ion conductors with oligoethers,  $(C_2H_4O)_nCH_3$ , and fluorosulfonates,  $CH_2CF_2SO_3^-M^+$  or  $OC_2H_4C_2F_4SO_3^-M^+$ , as pendant groups, are prepared from the linear correspondent polymer. Single-ion conducting polymer electrolytes yield the maximum Li transference number and are expected to provide greater depth of charge and discharge by preventing dc polarization at the electrodes. The highest conductivity obtained so far with single-ion conductors, in the presence of a plasticizer, is  $1.0 \times 10^{-3}$  S/cm at room temperature.

Unique polydiacetylene-based single ion conductors with high-room-temperature proton conductivity have been developed. The conductivity of these polymers is two orders of magnitude higher than that of Nafion under comparable experimental conditions. Diacetylene monomers carrying terminal sulfonic functional groups are polymerized by topochemical polymerization to yield proton-conducting, superionic molecular-tunnel electrolytes. In comparison with Nafion, these novel polymer electrolytes provide a larger surface density of proton-conducting sulfonic acid groups, promoting higher proton conductivity.

## ***In Situ* Raman Spectroscopy of Lithium Electrode Surfaces**

*H. Tachikawa (Jackson State University)*

The objective of this project is to characterize the surface layers on Li electrodes in nonaqueous electrolytes by electrochemical and Raman spectroscopic methods. The formation of passive layers on cathodically deposited Li has a strong influence on the rechargeability of Li electrodes. Characterizing the nature of the passive layers on the Li surface should provide information which is useful for improving the performance and cycle life of Li secondary batteries. Thin films of Li that were cathodically deposited on Ag electrodes were used in the *in situ* Raman spectroscopic studies of Li surfaces in nonaqueous solvents such as PC, mixed solvents (ester-based solvents and carbonate-based solvents), and polyethylene glycol 400 dimethyl ether (PEG400DME).

Raman spectroscopy showed the formation of passive films on the Li surface during the cathodic deposition of Li films in all of the above solvents except diethyl carbonate (DEC). The product from the reaction between Li and DEC dissolves in the electrolyte. However, the Raman spectra recorded at a smooth Ag surface after deposition of a thin Li film in a mixed solvent of DEC and methyl formate (MF) suggested the formation of a passive film on the Li surface. The passive films generally remained on the Li surface even after a positive potential was applied to the electrode. The frequencies of the Raman bands, which are due to the passive films, vary when different solvents are used. For example, the Raman spectra of the passive film recorded at a smooth Ag surface in 1 M  $LiClO_4$ /dimethyl carbonate (DMC) solution showed bands at 348, 449, 620, 891, and 1101  $cm^{-1}$ , but a mixed solvent of DEC and MF showed a couple of bands at 1085 and 1213  $cm^{-1}$ . The frequencies of these Raman bands changed when the electrode potential was changed between -0.3 and 3.0 V (*vs*  $Li^+/Li$ ). The above results suggest that the passive films generally remained on the Li surface during charging and discharging of Li, but its structure may change after several excursions to different potentials.

Cyclic voltammetry showed that PEG400DME has a wide potential window (more than 3 V) and is stable with Li. AC impedance measurements showed that the solution resistance of 0.5 M  $LiClO_4$ /PEG400DME is ~100 times greater than that of an aqueous solution with the same supporting electrolyte. A solid film of fullerene  $C_{60}$ , which could be used

as a cathode in Li rechargeable batteries, was examined in PEG400DME by both electrochemical and Raman spectroscopic methods. A thin film of  $C_{60}$  was prepared on a glassy carbon electrode surface. The cyclic voltammograms showed five redox peaks that suggested the formation of  $C_{60}^-$ ,  $C_{60}^{2-}$ ,  $C_{60}^{3-}$ ,  $C_{60}^{4-}$ , and  $C_{60}^{5-}$ . The  $C_{60}$  film did not dissolve in 0.5 M  $LiClO_4/PEG400DME$ , however,  $C_{60}$  anions can dissolve in the above solvent. The Raman spectra of a thin  $C_{60}$  film showed several bands in the range 250-1500  $cm^{-1}$  at open circuit. However, the above Raman bands disappeared when negative potentials were applied, because the thin fulleride film dissolved in the  $LiClO_4/PEG400DME$  solution at negative potentials. Further work is needed to find the proper conditions for stabilizing the fulleride anions.

## E. CROSS-CUTTING RESEARCH

Cross-cutting research is carried out to address fundamental problems in electrocatalysis, current-density distribution and gas evolution, solution of which will lead to improved electrode structures and performance in batteries and fuel cells.

### Analysis and Simulation of Electrochemical Systems

*J.S. Newman (Lawrence Berkeley Laboratory)*

The objectives of this project include the investigation of efficient and economical methods for electrical energy conversion and storage, development of mathematical models to predict the behavior of electrochemical systems and to identify important process parameters, and experimental verification of the completeness and accuracy of the models. The experiments and mathematical models are designed to identify the physical phenomena that govern these systems. The phenomena involved may include hydrodynamics, convective and diffusive mass transfer, ohmic potential drop, charge transfer, and heterogeneous and homogeneous kinetics. A thorough understanding of the interactions of the phenomena governing a given system leads to mathematical models that agree with experimental results and predict system behavior. The models are useful in the identification of important parameters, and they eventually aid in the design and scale-up of electrochemical systems. Although each electrochemical system has its own distinguishing features, all may be described by the fundamental principles of transport phenomena, reaction kinetics, materials science, and interfacial phe-

nomena. The computer implementation of numerical methods permits the complex interactions of these phenomena to be treated without the need for gross mathematical and physical approximations.

Improvements to the model of a SPE fuel cell were made to include the effects of electrode kinetics, mass transfer to the membrane-electrode interface, and thermal effects. The transport number of water in Nafion membranes over a wide range of water content was measured using a concentration cell. Water-management in the separator of a SPE fuel cell was examined in detail. Improvements to the polymer-electrolyte transport model will include the frequency response of the system. The model will be applied to other polymer electrolytes, such as PEO used in Li/polymer batteries. A comprehensive phenomenological model of the electrode/electrolyte interface will: *i)* elucidate dynamic changes with charge/discharge, *ii)* clarify formation of surface layers, and *iii)* form the basis for scale up and optimization of Li/polymer batteries.

The diffusion coefficient in concentrated sulfuric acid solutions was measured using an optical technique. The conductivity of sodium polysulfide melts as a function of concentration and temperature was measured. The results for both were analyzed and compared with previously obtained diffusion coefficient data.

Cathodic protection with parallel cylinders was examined by solving Laplace's equation with uniform current density on the cathode. Anodes should be placed so as to supply a uniform current density to the surface of the protected cathode to maintain it within a specified potential range relative to the adjacent electrolyte medium.

A model for electroless deposition was developed. Rotating-disk experiments have been conducted to measure the kinetic parameters necessary for a complete description of the systems.

A linear transform technique (based on a Kirchhoff transformation) has recently been discovered that allows one to solve for the potential and concentration distributions using Laplace's equation for the quasi-potential. This powerful technique will have applications in corrosion studies, etching systems, and microelectrodes, when convection can be neglected.

## PUBLICATIONS

1. A.C. West and J. Newman, "Current Distributions on Recessed Electrodes," *J. Electrochem. Soc.*, **138**, 1620 (1991).
2. J. Newman, "Cathodic Protection with Parallel Cylinders," *J. Electrochem. Soc.*, **138**, 3554 (1991).

3. D.R. Baker, M.W. Verbrugge and J. Newman, "A Transformation for the Treatment of Diffusion and Migration. Application to Stationary Disk and Hemisphere Electrodes," *J. Electroanal. Chem.*, 314, 23 (1991).
4. T.F. Fuller and J. Newman, "Experimental Determination of the Transport Number of Water in Nafion® 117 Membrane," LBL-31421 (1991).
5. J. Newman, *Electrochemical System*, 2nd edition, Prentice-Hall Inc., Englewood Cliffs, NJ (1991).

## Surface Layers on Battery Materials

R.H. Muller (Lawrence Berkeley Laboratory)

The purpose of this work is to advance the understanding of properties of surface layers on battery electrode materials that are important for the functioning of rechargeable galvanic cells with high-specific-energy and power capabilities, energy efficiency, charge retention, and cycle life. Means are sought to achieve superior, predictable properties of surface layers and to form them consistently in order to provide enhanced battery operation. Present studies are concerned with oxide formation on different metals, the cathodic deposition of Zn from alkaline media, and the corrosion of grid materials in lead/acid batteries.

Experimental observations of anodic oxide formation are made by *in situ* spectroscopic ellipsometry, Raman spectroscopy, elastic light scattering, and STM, in combination with electrochemical measurements and different *ex situ* techniques of surface analysis. Information concerning the composition and micromorphology of surface layers is used in theoretical models of nucleation, growth, and transformation of the layers. Spectroscopic ellipsometry is used to determine the spectral properties of surface materials and to derive wavelength-independent film structure parameters for which measurements at different wavelengths serve as independent monochromatic input. Film parameters are derived by the multi-dimensional optimization of optical models in which the difference between measurements and model predictions is minimized. Raman spectroscopy of surface layers is conducted with equipment that is sensitive enough to observe unenhanced emission. The sensitivity is achieved by use of a single monochromator, made possible by a multilayer filter for removing incident and laser plasma wavelengths and a channel plate detector for observing the entire spectrum simultaneously. STM is used to provide surface topography with atomic-level spatial resolution. Alignment

and coalescence of striations in cathodic metal deposition are investigated by the use of *in situ* video microscopy and TEM.

The transformation of nickel hydroxide to oxyhydroxide during the charging of Ni electrodes in alkaline solution has been found by STM to proceed by nucleation and growth of the oxidized phase from the metal surface. Efforts are underway to equalize the conductivities of the two nickel oxide phases in order to facilitate a more complete conversion of the hydroxide during charge. Different materials and processes are investigated to add dopants to the oxide phases. Similar processes will be used to reduce oxygen evolution during charging by increasing the oxygen overpotential.

Model calculations have shown that, because of the much higher conductivity of the oxidized material compared to that of the reduced material, the reaction front for the conversion propagates in a non-uniform fashion, leaving large amounts of unreacted material behind. At the end of charge, this material is shielded from further conversion by a thin surface layer of converted material. The model predictions have been confirmed by coulometric measurements and are consistent with optical measurements still in progress.

The surface modification of Pb and Pb-4% Sb alloy by the implantation of Ti atoms has been found to reduce the corrosion of these materials in sulfuric acid by up to 72-fold. The effect of the surface treatment on the corrosion reaction mechanism is under investigation, and tests with experimental battery plates will be conducted in cooperation with an industrial battery manufacturer.

## PUBLICATIONS

1. D.T. Schwartz and R.H. Muller, "Oxidation Films on Copper in Alkaline Media: Intensity-Modulated Photoelectrochemical and Raman Spectroscopy Studies," *Surf. Sci.*, 248, 349 (1991).
2. D.T. Schwartz and R.H. Muller, "Photoelectrochemical Evidence for Saturated Optical Absorption in Electrolytic Cuprous Oxide," *Appl. Phys. Lett.*, 55, 1739 (1991).
3. S.T. Mayer and R.H. Muller, "An *In Situ* Raman Spectroscopy Study of the Anodic Oxidation of Copper in Alkaline Media," LBL-30299 (1991).
4. L. McVay, "Studies of the Development of Mossy Zinc Electrodeposits from Flowing Alkaline Electrolytes," *Ph.D. Thesis*, LBL-30843 (1991).
5. D.P. Sutija, "Micro Scale Mass Transfer Variations During Electrodeposition," *Ph.D. Thesis*, LBL-30825 (1991).

## Application of Photothermal Deflection Spectroscopy to Electrochemical Interfaces

E.J. Cairns and F.R. McLarnon (Lawrence Berkeley Laboratory)

Photothermal Deflection Spectroscopy (PDS) is being used for *in situ* studies of electrochemical interfaces. PDS is a sensitive technique which measures the absorption spectrum of the electrode surface and simultaneously detects the concentration gradients formed in the electrolyte. The absorption spectrum can help identify reaction intermediates, which in turn help to determine the pathway by which the reaction occurs. The electrolyte concentration gradients contain information about the diffusion of reactants and products to and from the electrode. The sensitivity of these measurements is sufficiently high to detect reactions involving a single layer of molecules on the electrode surface.

PDS appears to be well-suited for the study of  $\text{CH}_3\text{OH}$  electrooxidation, which is a very slow reaction at the practical operating potentials of fuel-cell anodes. The rate-limiting step in the direct electrochemical oxidation of  $\text{CH}_3\text{OH}$  appears to be the transfer of oxygen (*i.e.*, from water) in the electrolyte to the Pt catalyst where it can react with  $\text{CH}_3\text{OH}$  to form  $\text{CO}_2$ . This overall reaction is very slow at the operating potential of a  $\text{CH}_3\text{OH}$  anode in a fuel cell. The process by which oxide layers form on Pt is being studied so that this rate-limiting step can be better understood. A model of this process, using the results of PDS measurements of electrolyte concentration gradients that accompany the formation and removal of oxide films on Pt, was developed.

The enhanced interest in electrocatalysis as a means for promoting electrochemical energy conversion reactions has increased the need for the development and improvement of new catalytic electrode materials as well as the need to better understand and elucidate the fundamental aspects of the electrocatalytic reaction mechanisms and interfacial phenomena. *In situ* spectroscopic techniques coupled with electrochemical measurements are ideal tools for use in the characterization of catalyst surfaces. By providing information concerning the Faradaic and diffusion processes involved in surface species adsorption/desorption and metal oxidation/reduction phenomena, PDS coupled with cyclic voltammetry experiments has been shown to be a useful technique for the *in situ* characterization of certain electrochemical interfaces.

PDS was used to elucidate the adsorption processes during the electroreduction and electrooxidation of organic molecules at catalytically

active porous Cu-based electrodes in alkaline and neutral methanolic solutions. The electrocatalytic hydrogenation of nitrobenzene on porous Devarda Cu (Raney-type metal) in comparison with smooth polycrystalline Cu has been examined. Porous and rough surfaces are usually optically dark and spectroscopic reflectance techniques are impractical. PDS has the significant advantage of being practical on dark electrodes, and *in situ* detection of the absorption spectra of organic molecular functional groups can be recorded in the infrared region, as well as in the UV-visible regions. Investigations in the infrared region in a thin-layer electrochemical cell showed that such detection should be possible with a powerful light source such as a tunable diode laser, rather than a conventional IR glow bar, without destroying or modifying the electrode interface under study. A Xe arc lamp was used in the investigations of nitrobenzene and its reduced intermediates in the UV-visible region. Present effort is directed toward the detection of various adsorbed species at different Cu interfaces.

### PUBLICATION

1. O. Haas, J. Rudnicki, F.R. McLarnon, and E.J. Cairns, "Mechanistic Investigations of Redox Polymer-Coated Electrodes Using Probe-Beam Deflection and Cyclic Voltammetry," *J. Chem. Soc. Faraday Trans.*, **87**, 939 (1991).

## Electrode Kinetics and Electrocatalysis of Methanol Electrooxidation

P.N. Ross (Lawrence Berkeley Laboratory)

The objective of this project is to develop an atomic-level understanding of the processes taking place in complex electrochemical reactions at electrode surfaces. Physically meaningful mechanistic models are essential for the interpretation of electrode behavior and are useful in directing the research on new classes of materials for electrochemical energy conversion and storage devices.

The relationship between the kinetics of electrode processes and the atomic structure of the electrode surface is being investigated. Processes under study include methanol-oxidation electrocatalysis by ordered alloys, oxygen electrocatalysis by organometallic complexes, and the corrosion of carbon electrode materials. Atomic-level structure determination is made by using a variety of techniques, depending on the material under study: low energy electron diffraction (LEED) for single crystals; high resolution electron microscopy for carbon electrode materials; and EXAFS for organometallic catalysts.

The Pt surfaces that are modified by selected adatoms constitute the most-active electrocatalysts for the direct electrooxidation of methanol. However, even the best of these catalysts suffers from very short lifetime and instabilities in performance. The basic mechanism of action of these adatoms remains speculative, and there is no rational basis for selecting one type of adatom over another. Recent work with single-crystal Pt surfaces has shown that there are two unexpected complications of surface structure on the catalytic effect of adatoms: *i*) the chemistry of the adatom is sensitive to the structure of the Pt surface, and *ii*) the specific adsorption of ions from the supporting electrolyte on both the Pt surface and the adatom has a strong effect on catalytic activity. An understanding of these complex interactions with methanol kinetics is lacking.

Studies of CO chemisorption and methanol electrooxidation on the [111] and [100] oriented single crystals of the isostructural (fcc) alloys of bulk stoichiometry  $MPt_3$  ( $M = Ti, Co$  and  $Sn$ ) were completed. The study of these alloys was ideal for separating ensemble effects from electronic effects in adsorbate bonding, because the surfaces of these ordered alloys formed by bulk truncation have the  $M$  atoms in fixed positions without any  $M-M$  pair sites. By varying  $M$  from  $Ti$  to  $Co$  to  $Sn$ , we can examine the effect of the  $d$  and  $s-p$  orbital contributions to the intermetallic bond on the binding energy of  $CO$ , which is the self-poisoning intermediate in methanol oxidation. A complication we had to contend with in these studies was the phenomenon of surface segregation, and the formation of surfaces that do not have the ideal structure and composition. The strength of the intermetallic bond was found to play a major role in determining the composition of the surface. In the very exothermic alloys,  $TiPt_3$  and  $SnPt_3$ , the thermodynamic tendency for the atom with the lower surface energy to be at the surface determined which of the two bulk planes forms the surface plane in the [100] orientation, either pure Pt ( $TiPt_3$ ) or 50%  $M$  ( $SnPt_3$ ). In  $CoPt_3$  where the intermetallic bonding is relatively weak, the lower surface energy of Pt produced pure Pt planes on both the [111] and [100] orientations. Photoemission and thermal desorption studies showed that the intermetallic bonding in all three alloys had only a small effect on the binding energy of  $CO$ , a decrease in the adsorption energy of 20 kJ/mol. The surprising invariance of adsorption energy on  $MPt_3$  surfaces having such a large variation in the  $d$ -orbital configuration of the  $M$  atom was attributed to the predominance of  $s-p$  orbital contributions to the intermetallic bond in these alloys. The weaker binding of  $CO$  on the  $MPt_3$  alloy surfaces had very little effect on the

potential for  $CO$  oxidation. However, the rate of methanol oxidation on either  $TiPt_3$  or  $SnPt_3$  surfaces was more than an order of magnitude lower than for a pure Pt of the same orientation. This inhibition was attributed to the loss of ensembles of Pt atoms having  $C_{3v}$  coordination due to the ordered substitution of  $Ti/Sn$  for Pt in the  $L1_2$  structure. These results support the reaction pathway postulated by the multiplet theory and indicate that the non-Pt adatom (presumably water activating) must be at relatively low ( $< 0.2$  ML) coverage for maximum activity.

The specific adsorption of anions in acid electrolytes containing sulfuric and hydrochloric acids was found to have a strongly inhibiting effect on the rate of methanol electrooxidation on both the [111] and [100] surfaces of Pt. The effect was much stronger in hydrochloric acid, requiring approximately three orders of magnitude higher concentration of sulfuric acid to achieve the same inhibiting effect (and surface coverage by adsorbed anion). The adsorption isotherms for  $Cl^-$  ions were measured by the emersion technique and *ex situ* AES analysis. The mechanism of inhibition appears to be similar in  $H_2SO_4$  and  $HCl$ . On Pt[111], anion adsorption was found to proceed in two stages, one coupled to hydrogen desorption producing a co-adsorbed state, and a second stage of adsorption at more anodic potentials into the anion adlattice from which hydrogen has been desorbed. The second-stage process on Pt[100] is different, occurring at more anodic potentials than on Pt[111] and concurrent with  $OH$  formation. Completion of the second stage of adsorption appears to produce the inhibition that causes a current peak to be observed in the voltammetry of methanol in acids containing these anions.

UPD of  $Cu$  in acids containing these electrolytes caused strong additional inhibition of methanol oxidation rate. The effect was attributed to induced anion adsorption on Pt atoms near the UPD  $Cu$  atoms due to a lowering of the local point of zero charge (pzc) by the  $Cu$  adatoms.

*In situ* Fe K-edge XANES has been employed to examine the axial coordination of  $\mu$ -oxobis [iron mesotetrakis (methoxyphenyl) porphyrin]  $(FeTMPP)_2O$ , irreversibly adsorbed on a high-area carbon substrate, Black Pearl (BP), as a function of the applied potential. Analysis of the XANES provides conclusive evidence that the coordination about  $Fe(3+)$  in the supported, fully oxidized macrocycle is remarkably different from that about  $Fe(2+)$  in the corresponding fully reduced macrocycle. In the adsorbed, oxidized state,  $(FeTMPP)_2O$  retains its  $\mu$ -oxo character and undergoes a two-electron reduction to yield predominantly four-coordinate square planar  $FeTMPP$  without axial ligation.

## PUBLICATIONS

1. A. Haner and P. Ross, "The Electrochemical Oxidation of Methanol on Tin-Modified Pt Single Crystal Surfaces," *J. Phys. Chem.*, **95**, 3740 (1991).
2. P.N. Ross, "Characterization of Alloy Catalysts for the Direct Oxidation of Methanol: A Critical Review," *Electrochim. Acta*, **36**, 2053 (1991).
3. A. Haner, P. Ross and U. Bardi, "The Surface Structure and Composition of the <111> and <100> Oriented Single Crystals of the Ordered Alloy Pt<sub>3</sub>Sn," *Surf. Sci.*, **249**, 15 (1991).
4. S. Kim, I.-T. Bae, M. Sandifer, P. Ross, R. Carr, J. Woicik, M. Antonio, and D. Scherson, "In-Situ XANES of an Iron Porphyrin Irreversibly Adsorbed on an Electrode Surface," *J. Amer. Chem. Soc.*, **113**, 9063 (1991).

## Effect of Electrocatalyst and Electrolyte Composition on Methanol/Air Fuel Cell Performance

E.J. Cairns and F.R. McLarnon (Lawrence Berkeley Laboratory)

The benefits of using CH<sub>3</sub>OH as a fuel where it undergoes direct electrochemical oxidation via an electrochemical step in a direct methanol fuel cell (DMFC) are offset by the difficulty in finding the appropriate combination of electrode structure, electrolyte composition, and catalyst that allow operation at useful power levels. The standard Pt electrocatalyst used in aqueous fuel cells is ineffective in oxidizing the poisons that form in the anodic CH<sub>3</sub>OH electrooxidation reaction, however additions of certain metals (*e.g.*, Ru) have shown promise in reducing anodic overpotentials. Also of importance is finding an electrolyte that simultaneously remains chemically invariant, is highly conductive, allows the fuel to dissolve to an appreciable extent, and is weakly adsorbing on the catalyst surface. Finally, the macro- and micro-structure of the electrode must maintain a stable electrolyte-gas interface, allow facile diffusion of reactants and products, and contain catalyst that is highly accessible to the reactants and electrolyte. The focus of this project is to optimize the DMFC anode structure for use with a Pt-Ru catalyst (the alloy is dispersed on graphitized carbon) and an intermediate-temperature (*i.e.*, 100-150°C) concentrated Cs<sub>2</sub>CO<sub>3</sub> electrolyte. Previous work has shown that carbonate electrolytes are chemically invariant when used in CH<sub>3</sub>OH/air fuel cells and have sufficiently high ionic

conductivity at moderately elevated temperatures. The physical structure of the electrode was varied by changing material parameters and processing conditions during its construction, and its current-potential curves were examined to correlate electrode performance with its structure.

Porous electrodes consisting of a gas diffusion layer (GDL) and a reaction layer (RL) were fabricated. The GDL consists of graphite paper wet-proofed with Teflon; it not only provides a pathway for the gaseous reactants and products, but also acts as physical support and current collector. The RL was made by mixing catalyst with Teflon to form a semi-hydrophilic pore structure, and was pressed onto the GDL. The metals loading can be varied by changing the thickness of the RL, or by changing the catalyst loading (typically 5-10 wt% metal) on the graphite, and ranged from 0.5 to 1.5 mg/cm<sup>2</sup>. Catalysts were also prepared by co-deposition from aqueous solutions of Pt and Ru salts (in a 1:1 Pt:Ru atomic ratio) onto the graphite, which was then reduced in a H<sub>2</sub> atmosphere. The catalyst and a Teflon suspension were ultrasonically mixed to form a slurry, which was pulled onto the GDL using a vacuum. The electrode was then hot-pressed in stages forming a bonded network of Teflon and graphite particles. A syringe drive and vaporizer delivered gaseous CH<sub>3</sub>OH to the anode at a rate approximately twice its stoichiometric value. The electrolyte composition ranged from 72 to 83 wt% (12-21 mol%) Cs<sub>2</sub>CO<sub>3</sub>, which allowed the cell to be operated at temperatures ranging from 80 to 120°C, at atmospheric pressure.

Initial work confirmed that dispersed Pt-Ru has a much higher catalytic activity for the oxidation of vaporized CH<sub>3</sub>OH than Pt alone. The anode overpotential was reduced by as much as 300 mV at 10 mA/cm<sup>2</sup> (in 72 wt% Cs<sub>2</sub>CO<sub>3</sub> at 120°C) with a Pt-Ru loading of 0.5 mg/cm<sup>2</sup>. However, the results indicated that, at this time, much of the catalyst is inaccessible to reactants due to poor wetting of the RL. Future work will concentrate on increasing wetting by changing the Teflon content of the RL and by varying the pressure and temperature during electrode fabrication. Concentrated Cs<sub>2</sub>CO<sub>3</sub> works well as an intermediate-temperature electrolyte for direct CH<sub>3</sub>OH oxidation with Pt-Ru catalyst, even though electrode structure has not yet been optimized for any particular electrolyte. Therefore, effort will continue to optimize the anode structure for this catalyst-electrolyte combination.

A cell operated with 72 wt% Cs<sub>2</sub>CO<sub>3</sub> exhibited much lower potential losses than a comparable cell operated with concentrated H<sub>3</sub>PO<sub>4</sub> electrolyte under similar conditions (80°C). We are continuing the optimization of the DMFC anode with Cs<sub>2</sub>CO<sub>3</sub> electrolyte and dispersed Pt-Ru catalyst.

## IV. AIR SYSTEMS RESEARCH

The objectives of this program element are to identify, characterize, and improve materials for air electrodes; and to identify, evaluate, and initiate development of metal/air battery systems and fuel-cell technology for transportation applications.

### A. METAL/AIR CELL RESEARCH

Metal/air cell research addresses O<sub>2</sub> electrocatalysis; bifunctional air electrodes, which are needed for electrically rechargeable Zn/air cells; and novel alkaline Zn electrode structures.

#### Electrocatalysts for Oxygen Electrodes

*E. Yeager (Case Western Reserve University)*

The overall objective of this research is to develop more effective electrocatalysts for O<sub>2</sub> reduction and generation which have high activity and long-term stability. Various electrocatalysts, including the transition-metal macrocycles and oxide catalysts, were evaluated to identify stable catalysts with much higher activity for both monofunctional and bifunctional air electrodes.

#### A. Transition Metal Macrocyclic Catalysts

*In Situ* FTIRRAS Studies of FeTsPc on Ag. The iron tetrasulfonated phthalocyanine (FeTsPc) complex adsorbed on an electrode surface at mono- or submonolayer level has high activity for the 4-electron reduction of O<sub>2</sub> to H<sub>2</sub>O or OH<sup>-</sup> in alkaline solutions. The orientation of the complex on the surface has a strong effect on the activity as well as reaction pathway for O<sub>2</sub> reduction. *In situ* surface-enhanced Raman spectroscopy (SERS) measurements obtained on Ag showed stretching modes involving C=C and C=N bonds of the macrocycle and provided evidence that the plane of the adsorbed TsPc complex is oriented at least partially perpendicular to the surface.

During 1991, *in situ* FTIRRAS measurements were conducted to obtain structural information on mono- or submonolayer adsorbed FeTsPc on Ag. The enhanced sensitivity was achieved by using a Dove prism (CaF<sub>2</sub>) as a window, instead of a flat window, which provides a higher incidence angle. Spectra at different potentials were obtained that have several derivative peaks corresponding to C=C or C=N vibra-

tion modes. This provides further evidence that the TsPc ring is oriented to the surface at a finite angle and is not parallel to the surface.

*Effect of Alcohols on Oxygen Reduction.* The effect of alcohols such as methanol (MeOH), isobutanol, and n-amyl alcohol on the electrocatalytic activity of transition-metal macrocycles for O<sub>2</sub> reduction was examined. These alcohols may change the structure of the interface and orientation of the adsorbed macrocycle on the electrode surface. The interest in methanol also lies in the need to develop MeOH-tolerant electrocatalysts for O<sub>2</sub> reduction in direct methanol fuel cells.

Voltammetric studies show evidence of co-adsorption of the alcohols along with the macrocycle on the electrode surface. The catalytic activity for O<sub>2</sub> reduction on CoTsPc, preadsorbed on an ordinary pyrolytic graphite (OPG) disk electrode, from an  $\sim 1 \times 10^{-4}$  M alkaline solution containing these alcohols is enhanced by an  $\sim 60$  mV positive shift of half-wave potential. Further, the presence of  $\sim 3$  M MeOH in acid or alkaline solutions has no short-term deleterious effect on O<sub>2</sub> reduction on the macrocycle, which exhibits negligible catalytic activity for MeOH oxidation.

Oxygen-reduction polarization measurements were also carried out using porous gas-fed electrodes based on pyrolyzed macrocycles including cobalt tetraazaannulene (CoTAA) and cobalt tetramethoxyphenyl porphyrin (CoTMPP) in 2.5 M H<sub>2</sub>SO<sub>4</sub> at 25 and 60°C. The presence of  $\sim 1$  M MeOH in the solution hardly affected the O<sub>2</sub> reduction performance. This is quite encouraging for the air electrode in DMFCs containing acid electrolytes.

*Solution-Phase Voltammetry.* Studies at CWRU have shown that the cyclic voltammetry of Co- and FeTsPc in aqueous acid or alkaline electrolytes on OPG disk electrodes correspond to the redox processes of the adsorbed macrocycle species and is not due to the dissolved species in solution. To separate the solution-phase redox peaks from those obtained for the adsorbed species on the electrode surface, voltammetric studies of these macrocycles have been carried out as a function of solvent. Solution-phase voltammetry of CoTsPc in CH<sub>3</sub>CN and (CH<sub>3</sub>)<sub>2</sub>SO containing tetraethylammonium perchlorate as the supporting electrolyte has been obtained on OPG, Au, and Pt disk electrodes. The currents associated with the solution-phase voltammetric peaks in organic solvents are low (on the order of a few  $\mu\text{A}/\text{cm}^2$ ). One possible explanation for this behavior may be that the

macrocycle is highly associated in organic solvents. This can lead to various complications which result in smaller, broader peaks.

A possible explanation for not obtaining the solution-phase voltammetric peaks of these macrocycles in aqueous solutions is based on the excess negative charge associated with the TsPc ring as a result of the ionized  $\text{SO}_3$  groups attached to the four aromatic rings. Another explanation may involve the edge-on adsorption of the macrocycle on the electrode surface. Under this condition the distance between the electrode surface and the solution-phase macrocycle molecule at the point of closest approach may be  $\sim 15 \text{ \AA}$ . It is difficult for the electrons to tunnel between the solution-phase macrocycle and the electrode over such a distance.

*STM and Atomic Force Microscopy (AFM) Studies.* During the last year, research was focused on the structural features of the adsorbed phthalocyanines using STM in the electrochemical environment. By using W or Pt-Ir needles, an image of a graphite surface immersed in deionized water was obtained with a hexagonal lattice with spacing of  $\sim 2.45 \text{ \AA}$  between the lattice planes. STM studies were also carried out in an aqueous solution of CoTsPc on highly ordered pyrolytic graphite (HOPG) using a new STM head with a two-stage amplifier (a trans-impedance preamplifier followed by an inverting amplifier) which results in a nearly 10-fold increase in signal-to-noise ratio. The background of HOPG could not be clearly seen and individual molecules of CoTsPc could not be observed probably because of the motion of the adsorbed molecules under the influence of the tip. An AFM was attached to the STM which is particularly attractive for *in situ* electrochemical studies because it does not involve the use of a tunneling current which otherwise might interact with the electrochemical system.

Efforts were made to obtain STM and AFM (*in situ*) images of CoTsPc adsorbed at mono- or submonolayer level on HOPG, but reproducible images free of artifacts have not been obtained thus far. Careful preparation of the tip is a very important factor in obtaining high resolution. The choice of substrate is also an important consideration for the study of the macrocycles. More *in situ* studies of the macrocycles adsorbed on various substrates are in progress with STM and AFM.

## B. Transition Metal Oxides as Catalyst and Support

Metallic oxides with the pyrochlore structure, particularly the stoichiometric lead-ruthenate  $\text{Pb}_2\text{Ru}_2\text{O}_{7-y}$ , are very active catalysts for both  $\text{O}_2$  re-

duction and generation in alkaline solutions with carbon supports, or in a self-supporting mode without high-area carbon as catalyst support. During the last year the lead-ruthenate pyrochlores were examined both as an electrocatalyst and as a support material to Pt for  $\text{O}_2$  reduction and generation in acid electrolyte (2.5 M  $\text{H}_2\text{SO}_4$  at 25 and  $60^\circ\text{C}$ ). Nafion 117 (DuPont) membrane material was pressed on the electrolyte side of the electrode. The performance for  $\text{O}_2$  reduction with the pyrochlore in gas-fed electrodes was found to be significantly lower in acid than that in alkaline solution (*i.e.*, over 200 mV more polarization at 10 mA/cm<sup>2</sup>). It was found that the  $\text{O}_2$ -generation reaction occurred almost as readily in acid as in alkaline solution, but with a higher Tafel slope,  $\sim 80 \text{ mV/decade}$  vs  $\sim 40 \text{ mV/decade}$ . The higher Tafel slope is not encouraging because the polarization at higher current densities becomes larger than that for the lower slope.

The  $\text{O}_2$ -reduction performance was much better with Pt-supported pyrochlore as compared with the pyrochlore alone. Approximately 10 wt% Pt was deposited using the method developed at Prototech. The  $\text{O}_2$ -generation performance was also significantly improved ( $\sim 40 \text{ mV/decade}$  Tafel slope) with the presence of deposited Pt. Thus there is some promise for the bifunctional  $\text{O}_2$  electrode in acid electrolyte using Pt supported on lead-ruthenate pyrochlore.

Transition metal oxides are of interest as alternative supports to carbon. Some of these oxides are quite stable in alkaline solution and have reasonable electronic conductivity. The effect of adsorbed CoTsPc on lithiated NiO for  $\text{O}_2$  reduction was investigated using the RDE and gas-fed electrode. In RDE experiments, mosaic single-crystal NiO and polycrystalline NiO grown on a metallic Ni disk were used. A significant enhancement of 2-3 fold in the  $\text{O}_2$  reduction kinetic current was observed in both 0.1 and 5.5 M KOH at room temperature. The presence of solution-phase CoTsPc was found to be necessary to obtain this effect. This indicates that the weak adsorption of CoTsPc on lithiated NiO is involved. However, Teflon-bonded gas-fed electrodes using this catalyst system gave poor performance. Possible reasons for this behavior are under examination, but it may be due mostly to the partial wetting of the electrode.

## PUBLICATIONS

1. S. Gupta, C. Fierro and E. Yeager, "The Effects of Cyanide on the Electrochemical Properties of Transition Metal Macrocycles for Oxygen Reduction in Alkaline Solutions," *J. Electroanal. Chem.*, 306, 239 (1991).

2. I.T. Bae, H. Huang, E.B. Yeager and D.A. Scherson, "In-Situ Infrared Spectroscopic Studies of Redox Active Self-Assembled Monolayers on Gold Electrode Surfaces," *Langmuir*, 7, 1558 (1991).
3. Z.Y. Zeng, S.L. Gupta, H. Huang and E.B. Yeager, "Oxygen Reduction on Poly(4-vinylpyridine)-Modified Ordinary Pyrolytic Graphite Electrodes with Adsorbed Cobalt Tetrasulfonated Phthalocyanines in Acid Solutions," *J. Appl. Electrochem.*, 21, 973 (1991).
4. S. Gupta, H. Huang and E. Yeager, "Studies on the Adsorption of Tetrasulfonated Phthalocyanines on Graphite Substrate," *Electrochim. Acta*, 36, 2165 (1991).

## Novel Concepts for Oxygen Electrodes in Secondary Metal/Air Battery

E. Rudd (Eltech Research Corporation)

The objective of this research is to develop improved bifunctional air electrodes for electrically rechargeable Zn/air cells. The successful development of bifunctional air electrodes depends on selecting electrochemically stable support materials and electrocatalysts for  $O_2$  reduction and evolution, and the fabrication of suitable porous structures that are capable of extended operation. The present program is directed at investigating the viability of graphitized carbons and metal oxides as supports for  $O_2$  electrocatalysts in bifunctional air electrodes.

The present program, initiated in October 1991, considers electrocatalyst supports based upon two carbon blacks, *i)* Shawinigan Black and *ii)* Cabot Monarch 120. After graphitization, these materials are fabricated into the active layers incorporating the following catalysts: *a)* nickel cobaltite,  $NiCo_2O_4$ , *b)* cobalt oxide,  $Co_3O_4$ , and *c)* the pyrochlores,  $Pb_2Ru_2O_7$  and  $Pb_2Ir_2O_7$ . The electrodes consist of two layers, the active layer and the gas supply layer, laminated together with a Ni-mesh current collector. The gas supply layer is the same for all electrodes and utilizes graphitized Shawinigan Black.

The following tasks are being addressed or completed:

*Task 1. Preparation of catalysts.* The catalysts have been prepared and characterized by x-ray diffraction analysis and BET surface area. X-ray analysis indicates that crystalline phases are produced in the syn-

thesis and the following surface areas were obtained:  $NiCo_2O_4$  (99  $m^2/g$ ),  $Pb_2Ru_2O_7$  (2.9  $m^2/g$ ), and  $Pb_2Ir_2O_7$  (1.9  $m^2/g$ ).

*Task 2. Preparation of carbon blacks.* The two carbon blacks have been graphitized and the following surface areas were obtained: Shawinigan black (73  $m^2/g$ ), graphitized Shawinigan black (51  $m^2/g$ ), Monarch 120 (31  $m^2/g$ ), and graphitized Monarch 120 (26  $m^2/g$ ).

*Task 3. Fabrication of electrodes.* Fourteen 8"  $\times$  8" electrodes have been fabricated.

*Task 4. Evaluation of electrodes in half cells.* Four Zn/air cells have been designed, fabricated, assembled, and prepared for electrochemical tests at MATSI.

## Transport in Zinc-Air Cells and Mathematical Modeling

J.W. Evans (Lawrence Berkeley Laboratory)

In previous work at LBL, a Zn/air cell that was mechanically recharged (the Zn being present as particles) was developed that met the anticipated requirements for EV applications. The cell operated by natural convection to drive the electrolyte through the cell, saving weight, reducing its complexity and cost, as well as eliminating the electrolyte pump. The major thrust of the continuing research is to transfer this concept to electrically rechargeable Zn/air cells and to provide a better understanding of its operation through mathematical-modeling studies.

A Zn/air cell with Zn present as a coating on a Cu foam substrate was invented by Ross at LBL. With the Zn in this form the cell can be cycled without the shape-change problem that is commonly associated with planar, monolithic Zn electrodes. In the original invention, the anolyte was pumped through the cell, which increased the cost, complexity, and weight of the battery while reducing its energy output. The objective of this research is to improve the performance of the cell, with the initial effort being directed at exploiting natural convection to achieve electrolyte flow, and thereby eliminating the need to pump the electrolyte.

The cost, complexity, and energy consumption that is associated with pumping the electrolyte in the Ross cell may be avoided by exploiting solutal natural convection. Such convection was successfully employed in an alternative (particulate Zn) cell which, under Simplified Federal Urban Driving Schedule (SFUDS) discharge, gave a performance that is pro-

jected to be 122 Wh/kg and 192 W/kg. Examination of this concept to the Ross cell is underway to obtain an improvement in its cell performance; this entails three steps: *i*) Discharge of laboratory cells designed to achieve electrolyte flow by natural convection. The performance of these cells is measured and compared with that of cells with pumped electrolytes. *ii*) Measurement of electrolyte velocities by laser-Doppler velocimetry. *iii*) Mathematical modeling of electrolyte flow, mass transport, reaction, and current flow in Zn/air cells with the objective of providing an interpretation of the experimental results and a tool for scale-up of the technology.

Laboratory cells were built for discharge of Zn/Cu foam electrodes under conditions where electrolyte flow is driven by natural convection. Discharge experiments under control of a microcomputer are permitting testing of the cells under SFUDS and other discharge regimens. The laser-Doppler velocimeter has been modified to measure the electrolyte velocity in cells and is giving the expected signals.

As a first step in mathematical modeling of the cell, an improved algorithm has been developed for convective diffusion of a solute in a porous electrode. The algorithm is a variant of the Lax-Wendroff algorithm. It yields more precise concentration profiles and this is important in modeling solutal natural convection where flow is driven by small differences in concentration. The existing mathematical model for discharge of cells with electrolyte flow driven by natural convection will be improved by *i*) incorporating an improved algorithm for convective diffusion in a porous electrode, *ii*) testing against experimental data for cell discharge characteristics, and *iii*) testing against electrolyte velocity measurements on laboratory cells.

## PUBLICATIONS

1. J.W. Evans, G. Savaskan and T. Huh, "Further Studies of a Zinc-Air Cell Employed in Packed Bed Anodes. Part I: Discharge," LBL-31679 (1991).
2. J.W. Evans, G. Savaskan and T. Huh, "Further Studies of a Zinc-Air Cell Employed in Packed Bed Anodes. Part II: Regeneration of Zinc Particles and Electrolyte by Fluidized Bed Electrodeposition," LBL-31680 (1991).
3. J.W. Evans and G. Savaskan, "Battery Using a Metal Particle Bed Electrode", *U.S. Patent 5,006,424*, April 1991.

## Development of Electrically Rechargeable Zinc/Air Cells

*E.J. Cairns and F.R. McLarnon (Lawrence Berkeley Laboratory)*

The bifunctional air electrode is the primary life-limiting component of electrically rechargeable Zn/air cells. Zinc electrode cycle lives of 600 and 800 cycles have been demonstrated with insoluble and soluble Zn electrodes, respectively. In comparison, bifunctional air electrodes are rarely reported to withstand more than 100 cycles at significant rates. The objectives of this project are to evaluate the performance and cycle-life of commercial bifunctional air electrodes in Zn/air cells and to develop improved bifunctional electrodes.

The study has focused on evaluating the BF-8 bifunctional air electrode from Electromedia, Inc. This electrode is a polytetrafluoroethylene (PTFE)-bonded graphitized carbon structure containing CoTMPP for O<sub>2</sub> reduction and Ni/Co spinel for O<sub>2</sub> evolution. These studies have been carried out in a cell with a reticulated, flow-through soluble-Zn negative electrode and an electrolyte composition of 45 wt% KOH and 40 g Zn<sup>2+</sup>/L. These cells were cycled with different constant-current rates as well as with the SFUDS variable-power discharge (Fig. 12). Approximately 25 cycles were achieved, regardless of the discharge rates used. A C/6 charge and a C/3 discharge yield extremely flat potential-time curves, with ~700 mV separating the charge and discharge potentials of the air electrode early in its life. Because there is no clear signal indicating the end of charge or end of discharge, these must be determined by integrating the charge (*i.e.*, counting coulombs) passed in the cycle test. End of life (capacity <60%) is caused by a premature end of discharge (cell voltage drops below 1.0 V) due to a rapid increase in the overvoltage of the air electrode. The reasons for this failure mode are under investigation.

The development of an in-house process for the production of bifunctional air electrodes is underway. Perovskites, pyrochlores and spinel oxides have been suggested as bifunctional electrocatalysts (those that catalyze both the reduction of O<sub>2</sub> during discharge and the oxidation of OH<sup>-</sup> to O<sub>2</sub> during charge). The perovskite, La<sub>0.6</sub>Ca<sub>0.4</sub>CoO<sub>3</sub>, with BET surface areas up to 18 m<sup>2</sup>/g was synthesized using the amorphous citrate precursor method. Catalyst powders were combined with graphitized carbon and PTFE in a dual-layer structure to make 25-cm<sup>2</sup> electrodes. Preliminary results with these electrodes are promising.

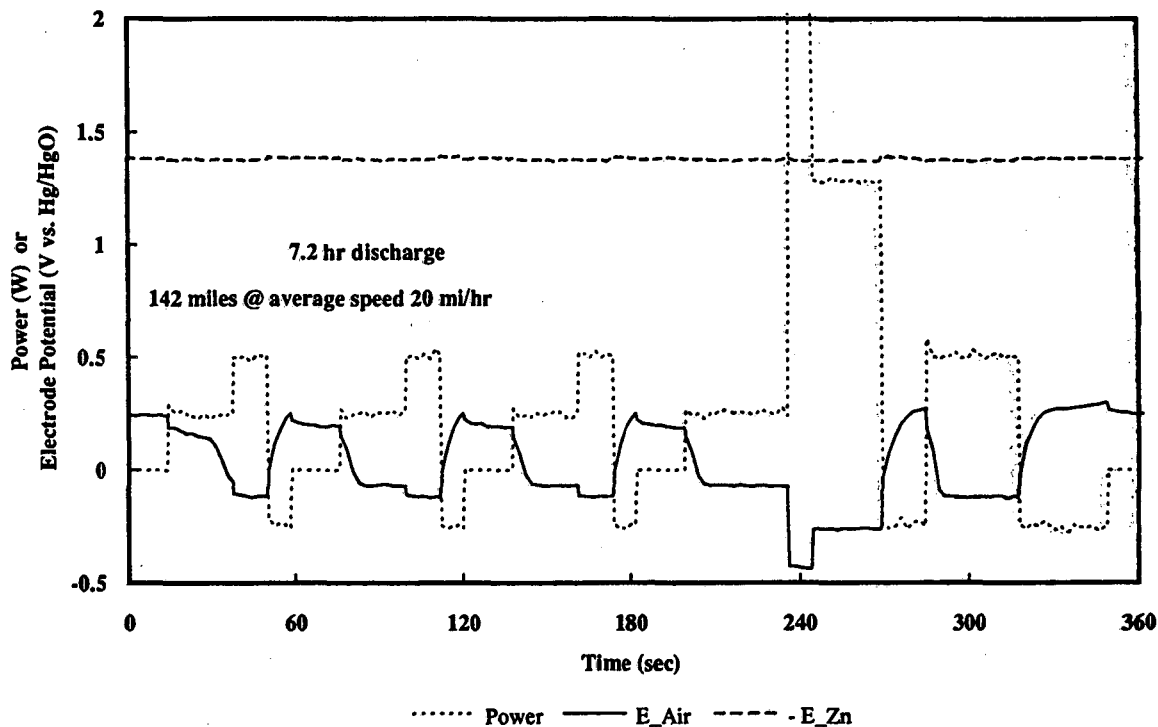


Figure 12. Discharge #6 of a 1.8 Ah Zn/air cell at SFUDS Repetition #40.

## B. FUEL CELL RESEARCH

Fuel cell research includes projects in several areas of electrochemistry: theoretical studies, fuel-cell testing, fuel processing, and fuel-cell component characterization.

### Fuel Cells For Renewable Applications

*S. Gottesfeld (Los Alamos National Laboratory)*

The primary focus of this program is to develop efficient and cost-effective proton exchange membrane (PEM) fuel cells for transportation applications. The specific goals of the program are to: *i)* reduce the cost of the Pt catalyst and ionomeric membrane, *ii)* increase the efficiency and power density of the PEM fuel cell, *iii)* optimize the system for operation on reformed organic fuels and air, *iv)* achieve stable, effi-

cient, long-term operation, and *v)* solve key technical issues that impede the development of DMFCs.

*Optimization of Membrane Electrode Assembly.* The work on membrane-electrode assemblies (MEA) has focused on their development based on "thin-film" catalyst layers. The catalyst layers are cast from blended solutions ("inks") to form thin films (~3- to 5- $\mu\text{m}$  thick) in which the catalyst and ionomer (e.g., Nafion) components are homogeneously mixed (no PTFE is used). This mixing greatly increases the ionomer contact with the catalyst sites, thereby rendering a high percentage of the catalyst sites active. As a result, much lower Pt loadings are possible, while maintaining an equivalent performance.

A "thin-film" catalyst layer was fabricated from a membrane and recast film in the  $\text{Na}^+$  form. The process involved casting the thin-film catalyst layer at elevated temperatures (185°C) from inks. The high-temperature cast results in a crystalline, robust form of the ionomer, while the  $\text{Na}^+$  form protects the

ionomer from degradation during heating. The impedance of fuel cells using these MEA is lower than that with membranes of the H<sup>+</sup> form. With Nafion 117, the impedance drops from more than 0.20 ohm-cm<sup>2</sup>, as obtained by hot pressing an impregnated gas diffusion electrode onto the membrane, down to 0.15 ohm-cm<sup>2</sup>. With the Dow membrane and membrane C, the impedances are <0.10 ohm-cm<sup>2</sup>. In addition, fuel cells with these membranes are more tolerant to adverse humidification conditions. The improvements are attributed to the enhanced interfacial continuity between the ionomers in the membrane and the catalyst layers, more facile H<sub>2</sub>O transport, and higher ionic conductivities. The performance obtained with membrane C and the Dow membrane are shown in Figures 13a and 13b, respectively. The performances

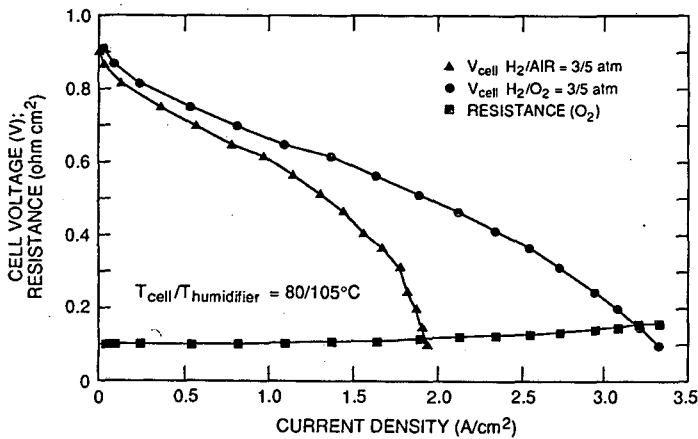


**Figure 13a.** Performance of a PEFC with a thin catalyst layer based on Pt/C catalyst bonded to the membrane. Loading - 0.17 mg Pt/cm<sup>2</sup>/electrode. The ionomeric membrane used here was membrane "C" (Chlorine Engineers, Japan).

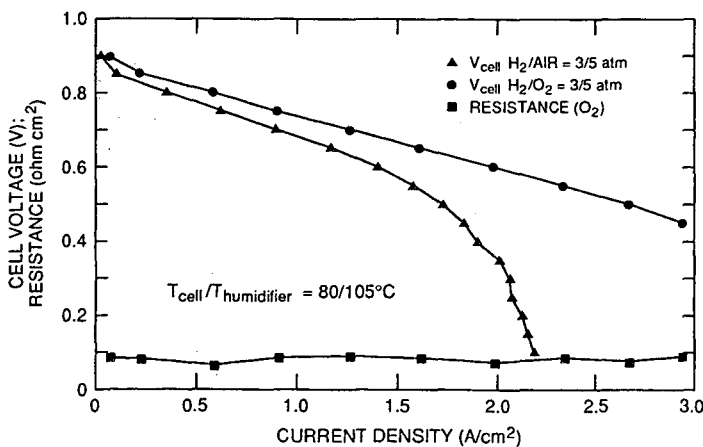


**Figure 13b.** Same as Fig. 13a for Pt loading of 0.13 mg Pt/cm<sup>2</sup>/electrode and an experimental Dow membrane.

of the cell with the Dow membrane is remarkable because it has a cathode loading of only 0.13 mg Pt/cm<sup>2</sup> and still achieves 1.3 W/cm<sup>2</sup>. It was also demonstrated that the anode performs satisfactorily using a thin-film catalyst layer electrode with as little as 0.03 mg Pt/cm<sup>2</sup>. The combination of these two values suggests that the power yield could approach 8 kW/g Pt. The Pt utilization in the new thin-film catalysts is compared in Figure 14 to catalyst utilization obtained with MEA obtained by earlier fabrication techniques.

**Water Management in MEAs.** Characterization of H<sub>2</sub>O uptake and H<sub>2</sub>O transport properties in fuel-cell membranes was expanded beyond Nafion 117 (hereafter referred to as N) to include Membrane C (900 EW) and Dow membrane XUS 13204.10 (800 EW), referred to as C and D below. The H<sub>2</sub>O uptake from liquid and vapor phases at room temperature, the H<sub>2</sub>O diffusion coefficients and the protonic conductivity as functions of H<sub>2</sub>O content, and the electroosmotic drag coefficients under experimentally realizable conditions were determined for the three membranes.

Table 1 summarizes the H<sub>2</sub>O uptake of the membranes in contact with liquid H<sub>2</sub>O following different drying conditions. After drying the membrane at room temperature, the membranes exhibit an H<sub>2</sub>O uptake from the liquid which is independent of the rehydration (immersion) temperature from 27°C to the boiling point. However, after baking at elevated temperature membrane D appears to show better H<sub>2</sub>O uptake than membranes N or C. This could be an advantage if the membrane is dehydrated, e.g., during hot-pressing of MEA, or if cell humidification is interrupted. The equilibrium H<sub>2</sub>O sorption from the vapor phase was essentially identical when normalized to

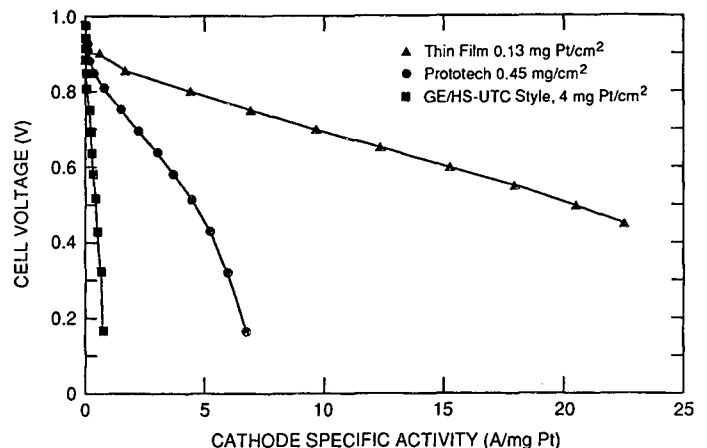


**Figure 14.** Comparison of specific Pt catalyst activities in PEFCs with three different types of Pt catalyst layers.

**Table 1. Water Uptake (H<sub>2</sub>O/SO<sub>3</sub>H) from Liquid Water**

Membrane	Dried at 27°C Rehydrated at 27°C	Baked at 105°C Rehydration Temperature		
		27	65	80
Nafion 117	21	12	15	16
Membrane C	21	11	15	17
Dow	25	17	21	23

the equivalent weight (EW) of the polymer, that is, membranes D and C (EW = 800-900) both take up more H<sub>2</sub>O per gram of polymer than N (EW = 1100). For each membrane, the amount of H<sub>2</sub>O uptake from the saturated vapor phase is less than that from the liquid phase.

Diffusion coefficients were determined for the various membranes using nuclear magnetic resonance (NMR). At 30°C, the diffusion coefficient of H<sub>2</sub>O was similar in the three membranes with the same  $\lambda$ .\* These values range from 0.2 to  $6 \times 10^{-6}$  cm<sup>2</sup>/s for partially hydrated membranes in contact with H<sub>2</sub>O vapor. Membranes D and C have somewhat higher H<sub>2</sub>O diffusion coefficients than membrane N in liquid H<sub>2</sub>O. In the case of membrane D, the higher diffusion coefficient is related to its higher H<sub>2</sub>O content. Data on the electroosmotic drag for the three membranes are reported in Table 2. These data suggest that the H<sub>2</sub>O drag is somewhat smaller in membrane D than in the other two membranes.

**Table 2. Water Drag by Protonic Current**

Membrane	Measured Drag, H <sub>2</sub> O/H <sup>+</sup> , 30°C
Nafion 117, 22 H <sub>2</sub> O/SO <sub>3</sub> H	2.5-2.9
Nafion 117, 11 H <sub>2</sub> O/SO <sub>3</sub> H	0.9
Membrane C, fully hydrated	2.6-4.1
Dow, fully hydrated	1.5

At 80°C, Nafion 117, 22 H<sub>2</sub>O/SO<sub>3</sub>H, has a H<sub>2</sub>O drag of 1.4-1.9.

\*  $\lambda = n(\text{H}_2\text{O})/n(\text{SO}_3\text{H})$  is the relative content of H<sup>+</sup> and H<sub>2</sub>O in the membrane.

The protonic conductivity of the three membranes as a function of H<sub>2</sub>O content, and the temperature dependence of the conductivity for immersed membranes, were also determined at 30°C. Both membranes C and D have a higher specific conductivity than N for  $\lambda \geq 5$ . However, the conductivity of these membranes decreases precipitously at lower H<sub>2</sub>O contents. For immersed samples of the three membranes, the temperature dependence of the protonic conductivity is similar, and thus, the differences in conductivities are maintained as the temperature is raised. The observed order of the conductivities of the membranes is D > C > N, which is apparently due to the difference in the equivalent weights, and to some extent to differences in their H<sub>2</sub>O content. The H<sub>2</sub>O uptake by immersed D is ~15% higher on a per sulfonate basis than the H<sub>2</sub>O uptake by N or C. This translates into a H<sub>2</sub>O diffusion coefficient that is 50 to 100% higher and a specific protonic conductivity ~50% higher for D. However, for partly hydrated membranes, the diffusion coefficients are similar for these membranes at a given state of hydration, with somewhat better conductivity exhibited over a range of H<sub>2</sub>O contents by membranes C and D.

Studies were initiated to elucidate the effects of the surface properties of the membrane on the dynamics of H<sub>2</sub>O uptake. The aim is to determine if a hydrophobic membrane "skin" exists that limits the sorption rate from the vapor phase. The contact angle between H<sub>2</sub>O and the perfluorosulfonate membrane surface was measured on membranes that were equilibrated with a H<sub>2</sub>O vapor of known activity. The results for N in Table 3 indicate that the membrane surface is hydrophobic even in contact with saturated H<sub>2</sub>O vapor. The samples with low H<sub>2</sub>O content exhibited advancing angles that are almost indistinguishable from those of completely dried membranes. After the membrane (locally) is exposed to liquid H<sub>2</sub>O, the surface become hydrophilic, as reflected by the much lower receding contact angles. These results suggest

**Table 3. Contact Angles for Water on Nafion 117 Membranes of Controlled Water Content**

Water Content	$P_{\text{H}_2\text{O}}/P_{\text{H}_2\text{O}}^0$	Contact Angle (Advancing/Receding)
0 H <sub>2</sub> O/SO <sub>3</sub> H	0	116/30
2 H <sub>2</sub> O/SO <sub>3</sub> H	0.14	115
4 H <sub>2</sub> O/SO <sub>3</sub> H	0.58	114
9 H <sub>2</sub> O/SO <sub>3</sub> H	0.82	107
14 H <sub>2</sub> O/SO <sub>3</sub> H	1.0 (vapor)	98/14

that the hydrophobic nature of the partly hydrated ionomeric membranes could result in a surface barrier to H<sub>2</sub>O uptake from the vapor.

*Single-Cell Endurance Testing.* Modifying the structure of the MEA resulted in a substantial improvement in the longevity of the PEM cell. One source of concern regarding the longevity of PEM cells is puncture of the membrane, however the experience at LANL has been that the probability is, in general, quite low. An exception is with thin membranes such as the 2-mil-thick experimental Nafion membrane. In this case, continuous cathode operation on neat O<sub>2</sub> was never achieved for more than a few hours, and it was always terminated by a puncture of the membrane. This problem was traced to the edge of the (Prototech) electrode which was hot pressed to the membrane during fabrication of the MEA. The edge is prone to puncturing because of a combination of strong deformation, or thinning, along the edge of the electrode. Also, during cell operation, this area of the membrane is exposed to the full chemical activity of the reactant gases because it lies in the flow field but is not covered by the gas-consuming electrode. This problem was solved by using a thin Teflon gasket in a new membrane/electrode/gasket assembly to prevent the sensitive area of the membrane from direct exposure to the reactant gases. Test results from this modified assembly have been very encouraging. A cell was operated at 5-atm O<sub>2</sub> (3-atm H<sub>2</sub>) for four weeks without failure. This is a very substantial improvement over previous attempts to operate under similar conditions. This success is important because it indicates that some of the concerns regarding the longevity of cells with thin membranes may no longer be an issue.

Testing of 50-cm<sup>2</sup> cells was started, employing a modified test station which enables smooth continu-

ous operation under life-test conditions. The major modification to the test station was to arrange for the automatic and continuous filling of the external humidification bottles with distilled H<sub>2</sub>O. The 50-cm<sup>2</sup> cells showed the best performance that was ever obtained at LANL in cells with such large active area. This result is particularly encouraging because the Pt loading was very low. One cell had a MEA that was prepared by catalyzing membrane C (Chlorine Engineers, Japan) with LANL's thin-film technique to achieve a Pt loading of 0.12 mg/cm<sup>2</sup> at the cathode and at the anode. The hardware consisted of graphite plates of significant porosity (Grade CGW, Union Carbide), which, based on previous work with 50-cm<sup>2</sup> cells, is essential to prevent cathode flooding. The initial O<sub>2</sub> polarization curve showed control by interfacial kinetics and membrane resistance only, *i.e.*, there were no transport losses up to 2 A/cm<sup>2</sup>. This is a significant achievement for a large (50 cm<sup>2</sup>) MEA operating with such low Pt loadings. The initial cell performance on air showed only marginal losses up to 1 A/cm<sup>2</sup>. The iR-corrected voltage at 1 A/cm<sup>2</sup> was 0.78 V on O<sub>2</sub>, and 0.72 V on air at the same total pressure (5 atm). The cell (high frequency) impedance varied between 0.18 ohm-cm<sup>2</sup> at low current densities and 0.20 ohm-cm<sup>2</sup> at the highest current densities (2.3 A/cm<sup>2</sup>).

A 50-cm<sup>2</sup> cell was run continuously during a 50-day test, except for four shut downs which occurred during repairs to the building power system. The crossover that was evident at termination was apparently caused by a punctured membrane. This may have been caused by the repeated shut downs, which resulted in some irreversible (local?) dehydration problems, and subsequent overheating and puncturing. The cell temperature was 80°C, humidifier temperatures was 105°C, and the gases were 5-atm air

and 3-atm  $H_2$ . The cell characteristic on  $H_2$ /air showed a continuous decline in performance during the 50 days of operation. The main conclusions from this test follow. *i*) The initial performance of cells with significant surface area ( $50 \text{ cm}^2$ ) and with extremely low Pt loadings are impressive ( $0.6 \text{ W/cm}^2$  on  $H_2$ /air). *ii*) The performance loss of 25% after 19 days and 50% after 41 days seems to be caused by changes in the cathode catalyst layer or cathode backing, which have been exacerbated by frequent shutdowns. *iii*) Changing the composition of the catalyst layer may solve the problem of gradual deterioration that is observed with this particular cell.

**PEM Fuel Cell Modeling.** A simple model for the catalyst layer was developed that successfully predicts the important characteristic features of the LANL PEM cells. The model is based on treating the catalyst layer as a composite "slab", with both uniform volume distribution of catalyst and specific protonic conductivity. The gas is supplied to one side of the slab, and the protons are supplied into the slab from the other (ionomeric membrane) side. The one-dimensional counter fluxes of  $O_2$  and  $H^+$  in the catalyst layer are the most fundamental feature of the model, which is schematically depicted in Figure 15. The  $O_2$  flux is characterized by average diffusion coefficient and solubility in the catalyst layer, the proton transport by an average conductivity, and the catalytic activity by catalyst surface area per unit volume of the slab. The complete behavior can be described by two dimensionless parameters:  $k_1 = nFC^*D/b\sigma$  and  $k_2 = A_v k_0 L^2/D$ , where  $nF$  is the number of coulombs per mole of  $O_2$ ,  $C^*$  is the solubility of  $O_2$  in

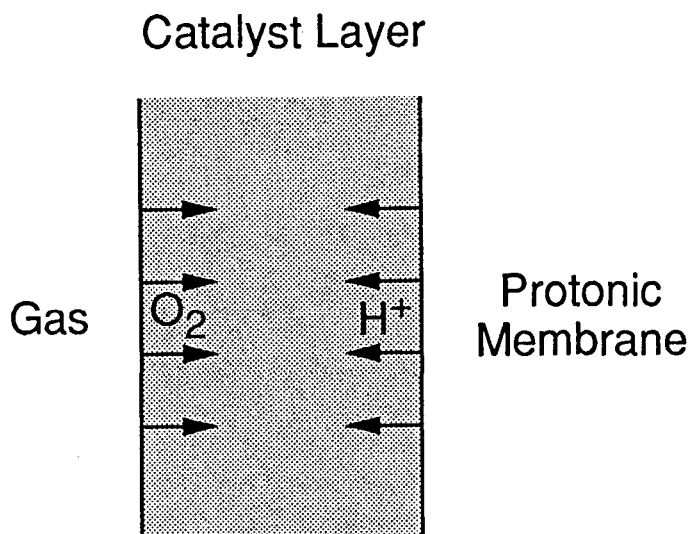


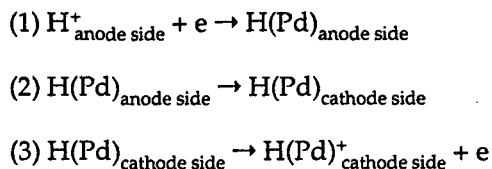
**Figure 15.** Schematic presentation of the counter fluxes of  $O_2$  and of protons in a cathode catalyst layer considered in modeling of this layer.

equilibrium with  $O_2$ ,  $\sigma$  is the average slab protonic conductivity,  $D$  is the average diffusion coefficient of  $O_2$ ,  $A_v$  is the catalyst surface area per unit volume,  $L$  is the thickness of the slab,  $k_0$  is the heterogeneous rate constant for the catalytic process, and  $b$  is the Tafel slope. At low overpotentials, the  $O_2$  concentration is quite uniform across the catalyst layer, the total voltage drop across the layer is small, and the current does not vary much with location. In contrast, at higher overpotentials, the model predicts a strong drop in  $O_2$  concentration within the slab, and in effect, only a part of the catalyst layer is utilized. If, at the same time, the protonic conductivity in the catalyst layer is limited, an increase in current density will result in an excessive increase of the effective overpotential.

The basic concept in this model is that counter fluxes of protons and  $O_2$  molecules determine the degree of utilization of the catalyst layer along its thickness dimension. The most important consequence is that combined  $O_2$  permeability/protonic conductivity limitations within the cathode catalyst have to be considered in evaluating air cathode performance at higher current densities.

**Direct Methanol Fuel Cells.** Development and testing of DMFCs were initiated, focusing on novel electrolytes, novel separators, and *in situ* catalyst cleansing. One of the major difficulties with direct methanol PEM fuel cell is the high solubility of methanol in the polymer. The effective separation of the methanol and the  $O_2$  compartments is considered to be the most critical problem in DMFCs based on membrane separators. Therefore, this issue was selected as the first to be investigated at LANL.

One possible solution to the crossover of methanol is to introduce a methanol-impermeable barrier between the two electrodes. This can be accomplished by effectively dividing the fuel cell into two parts, separated by a barrier impermeable to methanol, but which should allow a high rate of proton transfer. We recently experimented with a Pd foil as a separator that is perfectly impermeable to methanol, but which allows a high transport rate of hydrogen atoms. Protons can be transferred from the anode to the cathode compartments across a Pd foil by the following sequence:



The loss in cell voltage should be, in principle, quite small if the rates of the interfacial exchange  $H^+/H(\text{Pd})$  and H-atom transport in Pd metal are fast.

In the first experiment that was performed to test this idea, a 50- $\mu\text{m}$ -thick blackened Pd foil was painted with Nafion on both sides and hot pressed between two 5-mil (125- $\mu\text{m}$ ) thick pieces of membrane C, along with two conventional 5- $\text{cm}^2$  Prototech electrodes (0.35 mg Pt/ $\text{cm}^2$  plus 500 Å Pt film) impregnated with Nafion. To test the loss across the Pd foil, the cell was first tested  $\text{H}_2$  and  $\text{O}_2$ . The major impediment to the performance appeared to be the slow transfer of hydrogen across the Pd barrier, which is believed to be due to the low permeability of  $\text{H}_2$  in the Pd. Future efforts will consider precharging the Pd foil with  $\text{H}_2$ .

Research was started on alternative ionomeric membrane materials for use in PEM fuel cells operating on direct methanol at higher temperatures. A highly sulfonated poly(2,6-dimethyl phenylene oxide) was synthesized. The results so far indicate the following: *i*) sulfonation is facile, having achieved sulfonation levels up to roughly 80%; *ii*) the sulfonated product is  $\text{H}_2\text{O}$  soluble above 60% sulfonation; *iii*) a sample with 80% sulfonation is thermally stable, showing no weight loss by thermogravimetric analysis (TGA) below 210°C; and *iv*) membranes cast from solutions of this material tend to be brittle. The preliminary results indicate that well-hydrated sulfonated phenylene oxide have fairly high conductivity, on the order of  $10^{-2}$  S/cm at 30°C.

Another approach that may yield adequate protonic conductivity at elevated temperatures is to fabricate an interpenetrating networks of the materials of interest with Nafion. Silicon oxide phases were formed in a Nafion structure from siloxane monomers such as tetraethoxysilane and (3-aminopropyl)triethoxysilane. Physically, these membranes are significantly stiffer than Nafion membranes, and they also exhibit a low tendency to take up methanol. Finally, they appear to be thermally stable, with no weight loss observed by TGA up to 210°C. Further characterization of the properties of these new membranes is underway.

## PUBLICATIONS

1. T.A. Zawodzinski, M. Neeman, L.O. Sillerud, and S. Gottesfeld, "Determination of Water Diffusion Coefficients in Perfluorosulfonate Ionomeric Membranes," *J. Phys. Chem.*, **95**, 6040 (1991).
2. T.E. Springer, T.A. Zawodzinski, and S. Gottesfeld, "Polymer Electrolyte Fuel Cell Model," *J. Electrochem. Soc.*, **138**, 2334 (1991).
3. M.S. Wilson, T.E. Springer, T.A. Zawodzinski, and S. Gottesfeld, "Recent Achievements in Polymer Electrolyte Fuel Cell (PEFC) Research at Los Alamos National Laboratory," in *Proceedings of the 26th Intersociety Energy Conversion Engineering Conference*, August 4-9, 1991, Boston, MA, Vol 3., p. 636.
4. M.T. Paffett, W. Hutchinson, J.D. Farr, P. Pappin, J.G. Beery, S. Gottesfeld, and J. Feret, "The Physical and Chemical State of Phosphoric Acid Fuel Cell Assemblies After Long Term Operation: Surface and Near Surface Analysis," *J. Power Sources*, **36**, 137 (1991).
5. S. Gottesfeld, G. Maia, J.B. Floriano, G. Tremiliosi-Filho, E. Ticianelli, and E.R. Gonzalez, "Study of Thick Anodic Oxide Films On Pt By Spectroscopic Ellipsometry," *J. Electrochem. Soc.*, **138**, 3219 (1991).
6. T.E. Springer and S. Gottesfeld, "Pseudo-homogeneous Catalyst Layer Model for Polymer Electrolyte Fuel Cell," in *Proceedings of the Symposium on Modeling of Batteries and Fuel Cells*, The Electrochemical Society, **91-10**, 197 (1991).
7. T. Zawodzinski, T.E. Springer, J. Davey, J. Valerio and S. Gottesfeld, "Water Transport Properties of Fuel Cell Ionomers", in *Proceedings of the Symposium on Modeling of Batteries and Fuel Cells*, The Electrochemical Society, **91-10**, 187 (1991).
8. T.E. Springer, T. Zawodzinski and S. Gottesfeld, "Modeling Water Content Effects in Polymer Electrolyte Fuel Cells," in *Proceedings of the Symposium on Modeling of Batteries and Fuel Cells*, The Electrochemical Society, **91-10**, 209 (1991).
9. P. Allen, S. Conradson, I. Raistrick, S. Gottesfeld, J. Mustre de Leon, M. Lovato, and P. Stonehart, "Structure and Reactivity of the Metal Sites in Platinum-Based Electrocatalyst Clusters," in *Proceedings of the Workshop on X-ray Methods in Corrosion and Interfacial Electrochemistry*, The Electrochemical Society, **92-1**, 636 (1992).

## Advanced Chemistry and Materials for Fuel Cells

J. McBreen (Brookhaven National Laboratory)

The purpose of this work is to increase the understanding of electrocatalysis on a molecular level and to apply this knowledge to fuel cells. The goals of this project are to reduce the Pt requirements for PEM fuel cells, and to develop non-Pt catalysts for  $\text{O}_2$  reduction and catalysts for the direct oxidation of methanol. Work in 1991 included extended XAS studies of Pt/C in various acids and several Pt alloy catalysts.

*XAS Studies of Pt/C Electrocatalysts.* A comparative *in situ* XAS study was made on Prototech Pt/C electrocatalyst in 0.5 M H<sub>2</sub>SO<sub>4</sub> and 1 M HClO<sub>4</sub>. In the double-layer region, the XANES for the Pt catalyst in HClO<sub>4</sub> was almost identical to that for Pt foil. At positive potentials there was a substantial increase in the white line due to loss of d-band electrons on oxidation. At negative potentials there was a broadening of the white line that has been attributed to unoccupied antibonding states above the Fermi level. In 0.5 M H<sub>2</sub>SO<sub>4</sub>, there was a significant increase in the white line as compared to Pt foil, which is attributed to anion adsorption.

The XANES results in HClO<sub>4</sub> in the double-layer region indicate that neither Pt/H<sub>2</sub>O nor Pt/C interactions contribute significantly to the electronic structure of the Pt particles. This result and the EXAFS data indicate that these interactions are very weak. Table 4 summarizes the analysis of the EXAFS data for the first Pt-Pt shell in 0.5 M H<sub>2</sub>SO<sub>4</sub> and 1 M HClO<sub>4</sub>, at -0.24 and 0.3 V *vs* SCE. The data could be analyzed on the basis of a simple Pt-Pt model without accounting for Pt-C or Pt-O interactions. This is consistent with weak Pt-support interactions. The data are very similar in both acids and are consistent with 28 Å Pt particles. The Debye-Waller factor,  $\Delta\sigma^2$ , is higher in the double-layer region than in the hydrogen region. Recent x-ray scattering results on single-crystal Pt electrodes indicate that metal surfaces are reconstructed at negative potentials, and that the recon-

struction is lifted at more positive potentials. The same behavior may occur here. The ordered reconstructed surface would have less disorder and hence a lower Debye-Waller factor. The lifting of the reconstruction has implications for electrocatalysis of O<sub>2</sub> reduction and direct methanol oxidation.

*XAS Studies of Pt Alloy Catalysts.* *In situ* XAS results were obtained at the Pt L<sub>3</sub> and L<sub>2</sub> edges on carbon-supported Pt/Cr, Pt/Co, and Pt/Ni electrocatalysts. In the case of the Pt/Ni and Pt/Co alloys, XAS spectra were also obtained at the K edge for Co and Ni. Preliminary analysis of the XANES at the Pt L<sub>3</sub> edge indicates that alloying with Ni has a large effect on the d character of Pt. The results are consistent with an average positive charge for Ni and a negative one for Pt. Chromium, on the other hand, has little effect on the Pt d band structure. Preliminary EXAFS analysis indicates that the Ni forms a solid solution with Pt, with the Ni atoms substituting at Pt sites. The results so far indicate that XAS can yield an enormous amount of information on these catalysts.

#### PUBLICATION

1. J. McBreen, W.E. O'Grady, G. Tourillon, E. Dartyge, and A. Fontaine, "XANES Study of Underpotential Deposited Copper on Carbon-Supported Platinum," *J. Electroanal. Chem.*, **307**, 229 (1991).

Table 4. Structural Parameters from *In Situ* Pt EXAFS of Prototech Pt/C Data for First Pt-Pt Coordination Shell 0.5 M H<sub>2</sub>SO<sub>4</sub> and 1 M HClO<sub>4</sub>

Electrolyte	E(V <i>vs</i> SCE)	N	R (Å)	$\Delta\sigma^2$ (Å <sup>2</sup> )	$\Delta E^\circ$
1 M HClO <sub>4</sub>	0.30	10.66	2.75	0.00231	1
	-0.24	10.65	2.76	0.00161	1
0.5 M H <sub>2</sub> SO <sub>4</sub>	0.30	10.33	2.76	0.0023	0
	-0.24	9.97	2.76	0.00169	0

LAWRENCE BERKELEY LABORATORY  
UNIVERSITY OF CALIFORNIA  
TECHNICAL INFORMATION DEPARTMENT  
BERKELEY, CALIFORNIA 94720